



# Local Discontinuous Galerkin Methods to a Dispersive System of KdV-Type Equations

Chao Zhang<sup>1</sup> · Yan Xu<sup>1</sup> · Yinhua Xia<sup>1</sup>

Received: 21 May 2020 / Revised: 8 November 2020 / Accepted: 13 November 2020  
© Springer Science+Business Media, LLC, part of Springer Nature 2021

## Abstract

In this paper, we develop and analyze a series of conservative and dissipative local discontinuous Galerkin (LDG) methods for the dispersive system of Korteweg–de Vries (KdV) type equations. Based on a cardinal conservative quantity of this system, we design and discuss two different types of numerical fluxes, including the conservative and dissipative ones for the linear and nonlinear terms respectively. Thus, one conservative together with three dissipative LDG schemes for the KdV-type system are developed in our paper. The invariant preserving property for the conservative scheme and corresponding dissipative properties for the other three dissipative schemes are all presented and proven in this paper. The error estimates for two schemes are given, whose numerical fluxes for linear terms are chosen as the dissipative type. Assuming that the discontinuous piecewise polynomials of degree less than or equal to  $k$  are adopted, and conservative numerical fluxes are employed to discretize the nonlinear terms, we obtain a suboptimal a priori bound of order  $k$ ; yet in the case of dissipative fluxes, we obtain a slightly better bound of order  $k + \frac{1}{2}$ . Numerical experiments for this system in different circumstances are provided, including accuracy tests for two kinds of traveling waves, long-time simulations for solitary waves and interactions of multi-solitary waves, to illustrate the accuracy and capability of these schemes.

**Keywords** Korteweg–de Vries system · Local discontinuous Galerkin methods · Conservative and dissipative · Error estimates

---

Yan Xu: Research supported by Science Challenge Project TZT2019-A2.3, NSFC Grant Nos. 11722112, 12071455. Yinhua Xia: Research supported by National Numerical Windtunnel Project NNW2019ZT4-B08, NSFC Grant No. 11871449.

---

✉ Yan Xu  
yxu@ustc.edu.cn

Chao Zhang  
zc56@mail.ustc.edu.cn

Yinhua Xia  
yhxia@ustc.edu.cn

<sup>1</sup> School of Mathematical Sciences, University of Science and Technology of China, Hefei 230026, Anhui, People's Republic of China

## 1 Introduction

In this paper, we introduce and analyze local discontinuous Galerkin methods (LDG) designed to approximate solutions of the following system of Kortweg-de Vries (KdV) type equations, which we call as the KdV-type system in short, taking the form

$$\begin{cases} u_t + u_{xxx} + R(u, v)_x = 0, \\ v_t + v_{xxx} + S(u, v)_x = 0, \end{cases} \tag{1.1}$$

The above two equations are coupled by the nonlinear terms  $R(u, v)$  and  $S(u, v)$ , which are taken to be homogeneous quadratic polynomials, namely

$$R = Au^2 + Buv + Cv^2, \quad S = Du^2 + Euv + Fv^2, \tag{1.2}$$

where  $A, B, \dots, F$  are given real coefficients and the variables  $u(x, t)$  and  $v(x, t)$  are time-dependent real-valued functions.

Well-posedness and many important properties about the KdV-type system (1.1) are studied and presented in [1,4,6,11,12]. In [5], Bona et al. provide a thorough discussion of the extant literature regarding the KdV-type system (1.1). We list several useful facts discussed therein which are useful in the analysis to follow. Following the theories developed for the single KdV equation, the KdV-type system (1.1) can be proven locally well-posed in the Sobolev spaces  $H^s(\mathbb{R}) \times H^s(\mathbb{R})$  for any  $s > -\frac{3}{4}$ . For  $s \geq 0$ , the following quantity

$$\mathcal{H}(u, v) = \int_{\mathbb{R}} (au^2 + buv + cv^2) dx, \tag{1.3}$$

is invariant in time, where the constants  $a, b, c$  are any nontrivial solutions of the system

$$\begin{cases} 2Ba + (E - 2A)b - 4Dc = 0, \\ 4Ca + (2F - B)b - 2Ec = 0. \end{cases} \tag{1.4}$$

Furthermore, when the quadratic form  $\mathcal{T}(x, y) = ax^2 + bxy + cy^2$  is positive-definite, i.e.,

$$4ac - b^2 > 0, \tag{1.5}$$

the system (1.1) can be extended to be globally well-posed if  $s \geq 0$ . Although the well posedness in  $H^s(\mathbb{T})$  ( $\mathbb{T} = \mathbb{R}/\mathbb{Z}$  is the one-dimensional torus) has not been dealt with, the Bona–Smith argument in [6] with some a priori  $H^1(\mathbb{T})$ -bound deduces global well posedness for  $s \geq 1$  when  $4ac - b^2 > 0$ , and such a conclusion on the one-dimensional torus for  $s \geq 1$  is sufficient for our analysis in this paper. In addition, the system (1.1) admits some special solitary-wave solutions, which are termed as the proportional solitary waves in [4], and we will give detailed introductions about it in the future section of numerical experiments.

In our study, we will focus on the design and analysis of numerical schemes to solve the system (1.1). Although methods of the KdV equation are abundant, the LDG framework in this paper is mainly enlightened by the contributions towards (local) discontinuous Galerkin (DG) methods, especially the work in [3,7,22,27,31]. The LDG methods for the KdV and other equations with high order derivatives are initially introduced in [27] by Yan and Shu. And the  $L^2$ -error estimates for the semi-discrete LDG method to the KdV equation are presented by Xu and Shu in [22], and one of our key error estimates in this paper is mainly guided by their work. Then Cheng and Shu in [7] proposed a new DG method to time dependent partial differential equations with higher order spatial derivatives. Besides, the conservative

DG methods are presented in [3,31] to solve the generalized KdV (gKdV) equation

$$u_t + (u^{p+1})_x + \epsilon u_{xxx} = 0,$$

where  $p$  is nonnegative integer and  $\epsilon$  is a nonzero parameter, and their ideas of constructing and analyzing the weak forms of nonlinear terms in the gKdV equation give us important inspiration to design schemes for coupled nonlinear terms of system (1.1). And in [15,16], the authors present some *a posteriori* error estimates for DG and LDG methods to the generalized KdV equation. More recently, Bona and collaborators in [5] start to embark on numerical approximations to this KdV-type system (1.1): they construct a continuous Galerkin scheme which can preserve the invariant  $\mathcal{H}$  and provide the error estimates with a suboptimal  $k$ -th order of accuracy ( $k$  is the degree of polynomial). Enlightened by their contributions, we set about studying the LDG method applied to this KdV-type system, and some strategies and skills used in [5] to handle such delicate system are also adopted in our work. Other than the work on DG/LDG methods, we also introduce some useful tools and concepts for the symmetric/symmetrizable systems of conservation laws, such as the “E-fluxes” in [14] and corresponding important properties studied in [29,30]. This is because there exists some “hidden” symmetrizable property of the system (1.1) and it will be in detail explained in this paper. By these useful tools, we could provide some higher accuracy with  $(k + \frac{1}{2})$ th order for two dissipative schemes, and these results are consistent with the accuracy order obtained in [22] of the similar LDG scheme to the KdV equation.

The LDG method discussed in present paper is an extension of the discontinuous Galerkin (DG) method to solve partial differential equations (PDEs) containing higher than first order spatial derivatives, using discontinuous piecewise polynomials as numerical solutions and test functions in the spacial variables. The LDG method was first constructed by Cockburn and Shu [10] in solving nonlinear convection–diffusion equations, which was inspired by the efficient numerical experiments of Bassi and Rebay [2] for simulating the compressible Navier–Stokes equations. In the procedure of the LDG method, higher order derivatives are rewritten into a first order system and applied with DG method subsequently. The cardinal technique in the LDG method is the design of the so-called numerical fluxes. The literatures on designing and analyzing the LDG schemes for different kinds of equations are quite plenty, and we suggest that the readers consult [10,21,23–28,31] and the references therein. These contributions about the LDG method could supply rich and efficient guidance for us when encountering new equations or similar problems.

The extremely local, element based discretization in the DG method is effectively favorable for parallel computing and retaining high-precision on unstructured meshes. Particularly, DG methods are well suited for *hp*-adaptation, which consists of local mesh refinement and the adjustment of the polynomial order in individual elements. The LDG schemes for the KdV-type system (1.1) in present paper keep all these good properties.

Our paper is organized as follows: in Sect. 2, notations and other preliminary materials, such as the function spaces and their norms are first introduced. We also construct and analyze a new kind of numerical fluxes with two variables, together with some operators and forms for the linear and nonlinear terms for the KdV-type system. In Sect. 3, four different LDG schemes are designed, including one conservative scheme and three dissipative ones. The stability analysis with respect to the quantity  $\mathcal{H}$  defined in (1.3) for these four schemes are presented in Sect. 4. Section 5 comprises error estimates for two dissipative schemes with different numerical fluxes chosen for the nonlinear terms. In Sect. 6, we implement these numerical approaches to some examples for the KdV-type system to illustrate their accuracy and capability. In particular, the long-time simulation of solitary-wave solutions and the

interactions of multi-solitary waves are numerically validated. Concluding remarks are given in Sect. 7.

## 2 Notations and Definitions

Based on the LDG method, we will design several different numerical schemes for the KdV-type system (1.1). For the sake of concision, we present and list here some necessary notations, definitions and corresponding preliminary materials which will be used throughout the paper.

### 2.1 Notations, Function Spaces and Norms

#### 2.1.1 The Meshes

Let  $I = [0, 1]$  denote the spatial domain for the methods and the system (1.1), and  $\mathcal{T}_h$  be the partition of  $I$  with the cells  $I_j = [x_{j-\frac{1}{2}}, x_{j+\frac{1}{2}}]$  for  $j = 1, \dots, N$ , where

$$0 = x_{\frac{1}{2}} < x_{\frac{3}{2}} < \dots < x_{N+\frac{1}{2}} = 1.$$

The center of the cell is  $x_j = \frac{1}{2}(x_{j-\frac{1}{2}} + x_{j+\frac{1}{2}})$  and the mesh size is denoted by  $h_j = x_{j+\frac{1}{2}} - x_{j-\frac{1}{2}}$  with  $h = \max_{1 \leq j \leq N} h_j$  being the maximum cell size. The mesh is assumed to be regular, which means the ratio between the maximum and minimum mesh sizes keeps bounded in the mesh refinements.

#### 2.1.2 Function Spaces and Norms

We introduce the Sobolev spaces  $W^{s,p} = W^{s,p}(I)$  together with their usual norms, and also use  $H^s = H^s(I)$  to denote  $W^{s,2}$ . Besides,  $C(I)$  will denote the spaces of functions which are continuous on  $I$ . In particular, we also introduce function spaces  $C_{per}(I)$  which are continuous and periodic on  $[0, 1]$  with extra restrictions on  $x_{\frac{1}{2}}$  and  $x_{N+\frac{1}{2}}$ , namely

$$C_{per}(I) = \{u(x) \in C(I) : u(x_{\frac{1}{2}}) = u(x_{N+\frac{1}{2}})\}.$$

In addition, we introduce the broken Sobolev spaces  $W^{s,p}(\mathcal{T}_h)$ , which are finite Cartesian products of the standard Sobolev spaces  $W^{s,p}(I_j)$  on all cells in  $\mathcal{T}_h$ . When  $p = 2$ ,  $H^s(\mathcal{T}_h)$  is always used to denote  $W^{s,2}(\mathcal{T}_h)$ . In particular, norms of  $W^{s,p}(\mathcal{T}_h)$  with  $p = 2, \infty$  are given by

$$\|u\|_{W^{s,2}(\mathcal{T}_h)} = \|u\|_{H^s(\mathcal{T}_h)} = \left( \sum_{j=1}^N \|u\|_{H^s(I_j)}^2 \right)^{\frac{1}{2}}, \quad \|u\|_{W^{s,\infty}(\mathcal{T}_h)} = \max_{1 \leq j \leq N} \|u\|_{W^{s,\infty}(I_j)}.$$

In the case  $s = 0$  with the interval  $I$  being clear from context, we would like to use the norms  $\|u\|$  and  $\|u\|_\infty$  to connote  $\|u\|_{L^2(\mathcal{T}_h)}$  and  $\|u\|_{L^\infty(\mathcal{T}_h)}$  respectively. Furthermore, it is necessary in our analysis to define the function space  $H^s_{per}(\mathcal{T}_h) = C_{per}(\mathcal{T}_h) \cap H^s(\mathcal{T}_h)$ , where  $C_{per}(\mathcal{T}_h)$  connotes the periodic and piecewise continuous functions with possible discontinuity on the element interfaces.

### 2.1.3 The Finite Element Spaces

Now we choose the following discontinuous piecewise polynomial space as the finite element space

$$V_h = \left\{ v(x) : v(x) \in P^k(I_j), \text{ for } x \in I_j, \quad j = 1, \dots, N \right\}, \tag{2.1}$$

where  $P^k(I_j)$  denotes the set of polynomials of the degree up to  $k$  in each cell  $I_j$ . It transpires that the functions belonging to  $V_h$  could be discontinuous on the element interfaces.

The solution of the numerical scheme is denoted by  $u_h$ , which belongs to the finite element space  $V_h$ . We denote the values of  $u_h$  at  $x_{j+\frac{1}{2}}$  by  $(u_h)_{j+\frac{1}{2}}^+$  and  $(u_h)_{j+\frac{1}{2}}^-$ , from the right cell  $I_{j+1}$  and the left cell  $I_j$ , respectively. The usual notations

$$[u_h]_{j+\frac{1}{2}} = (u_h^+ - u_h^-) \Big|_{j+\frac{1}{2}}$$

and

$$\{u_h\}_{j+\frac{1}{2}} = \frac{1}{2}(u_h^+ + u_h^-) \Big|_{j+\frac{1}{2}}$$

are also introduced to connote the jump and mean of the function  $u_h$  at  $x_{j+\frac{1}{2}}$ , respectively. When the context is clear, the unadorned notations  $[u_h]$  and  $\{u\}$  will be used.

## 2.2 Preliminary Materials and Definitions

In design of the weak formulation of LDG schemes for the KdV-type system (1.1), different kinds of numerical fluxes for nonlinear and linear terms will be discussed, thus in this subsection, we beforehand present some concise forms and operators according to different numerical fluxes together with some important properties.

### 2.2.1 Properties of Nonlinear Terms

Denote  $f(u, v) = uv$ , then nonlinear terms in (1.1) can be written as

$$R(u, v) = Af(u, u) + Bf(u, v) + Cf(v, v), \tag{2.2}$$

$$S(u, v) = Df(u, u) + Ef(u, v) + Ff(v, v). \tag{2.3}$$

According to the above nonlinear terms, two kinds of preliminary materials are designed and analyzed in this part.

- Conservative-type notations and definitions.** Assuming  $u$  and  $v$  are functions defined in  $I$ , we construct a kind of conservative numerical flux for  $f(u, v)$  as

$$\hat{f}(u, v) = \frac{1}{6} (2u^+v^+ + u^+v^- + u^-v^+ + 2u^-v^-), \tag{2.4}$$

herein the ‘‘hat’’ terms are the so-called numerical fluxes aforementioned. Then the numerical fluxes for  $R$  and  $S$  can be described as

$$\widehat{R}_c(u, v) = A\hat{f}(u, u) + B\hat{f}(u, v) + C\hat{f}(v, v), \tag{2.5}$$

$$\widehat{S}_c(u, v) = D\hat{f}(u, u) + E\hat{f}(u, v) + F\hat{f}(v, v). \tag{2.6}$$

**Lemma 2.1** (The properties of  $\hat{f}$ ) *The numerical flux  $\hat{f}$  defined in (2.4) possesses the following properties*

1. For  $u, v \in C_{per}(I)$ ,  $\hat{f}$  is consistent with  $f$ , i.e.,

$$\hat{f}(u, v) = uv. \tag{2.7}$$

2. For  $u, v, w$  are functions defined in  $I$ , there holds an identity

$$[uvw] = \hat{f}(u, v)[w] + \hat{f}(v, w)[u] + \hat{f}(w, u)[v]. \tag{2.8}$$

**Proof** 1. The consistence can be obviously obtained when  $u, v$  are both continuous and periodic at each node of  $\mathcal{T}_h$ .

2. This equality is a direct result of the definition of  $\hat{f}$  and some basic algebraic manipulations.

□

**Remark 2.2** When taking  $w = u$  in (2.8), we immediately obtain an obvious but important relation

$$[u^2v] = 2\hat{f}(u, v)[u] + \hat{f}(u, u)[v]. \tag{2.9}$$

**Remark 2.3** In a general sense,  $\hat{f}(u, v)$  is a two-component extension of the conservative flux for  $f(u) = u^2$  presented in [3,31], namely

$$\hat{f}(u, u) = \frac{1}{3} \left( (u^+)^2 + u^+u^- + (u^-)^2 \right) = \frac{[F(u)]}{[u]}, \tag{2.10}$$

where  $F(u) = \int_0^u s^2 ds$  and assume  $[u] \neq 0$ . This is a direct result when we choose  $v = u$  in (2.4).

The definition of the conservative numerical flux  $\hat{f}$  in (2.4) motivates the conservative trilinear form  $\mathcal{N}_c$ : for  $u, v, \rho \in H^1(\mathcal{T}_h)$ ,

$$\mathcal{N}_c(u, v; \rho) = - \sum_{j=1}^N (uv, \rho_x)_{I_j} - \sum_{j=1}^N \left( \hat{f}(u, v)[\rho] \right)_{j-\frac{1}{2}}, \tag{2.11}$$

where  $(\cdot, \cdot)_{I_j}$  denotes the  $L^2$ -inner product over the interval  $I_j$ . By virtue of the Riesz Representation Theorem, we define the nonlinear operator  $\mathcal{N}_c : H^1(\mathcal{T}_h) \times H^1(\mathcal{T}_h) \rightarrow V_h$  as follows

$$(\mathcal{N}_c(u, v), \rho) = - \sum_{j=1}^N (uv, \rho_x)_{I_j} - \sum_{j=1}^N \left( \hat{f}(u, v)[\rho] \right)_{j-\frac{1}{2}}, \quad \text{for } \forall \rho \in V_h, \tag{2.12}$$

where the unadorned notation  $(\cdot, \cdot)$  denotes the  $L^2$ -inner product over the domain  $[0, 1]$ .

**Lemma 2.4** (The properties of  $\mathcal{N}_c$ ) *The trilinear form defined in (2.11) possesses the following properties*

1.  $\mathcal{N}_c$  is consistent in the sense that,

$$\mathcal{N}_c(u, v; \rho) = ((uv)_x, \rho), \quad \text{for } u, v \in H^1(I) \cap C_{per}(I), \quad \rho \in V_h. \tag{2.13}$$

2. For  $u, v, w \in H^1(\mathcal{T}_h)$ ,

$$\mathcal{N}_c(u, v; w) + \mathcal{N}_c(w, u; v) + \mathcal{N}_c(v, w; u) = 0. \tag{2.14}$$

3. For  $u, v \in H^1(\mathcal{T}_h)$ ,

$$\mathcal{N}_c(u, v; u) = -\frac{1}{2}\mathcal{N}_c(u, u; v). \tag{2.15}$$

4. For  $u \in H^1(\mathcal{T}_h)$ ,

$$\mathcal{N}_c(u, u; u) = 0. \tag{2.16}$$

**Proof** 1. For  $u, v \in H^1(I) \cap C_{per}(I)$ , the conclusion (2.13) is easy to be obtained by integration by parts, periodicity and continuity at each node

$$\mathcal{N}_c(u, v; \rho) = ((uv)_x, \rho) + \sum_{j=1}^N \left( (uv - \hat{f}(u, v))[\rho] \right)_{j-\frac{1}{2}} = ((uv)_x, \rho).$$

- 2. Since  $u, v, w \in H^1(\mathcal{T}_h)$ , integration by parts, applying periodic boundary conditions and (2.8), the desired equality (2.14) comes out obviously.
- 3. Property (2.15) follows by taking  $w = u$  in (2.14) and the symmetry of the first two components of  $\mathcal{N}_c$ .
- 4. Take  $v = u$  in (2.15), we get that

$$\mathcal{N}_c(u, u; u) = -\frac{1}{2}\mathcal{N}_c(u, u; u).$$

□

**Remark 2.5** When we further define the nonlinear operators  $\mathcal{R}_c$  and  $\mathcal{S}_c$  based on the definition of operator  $\mathcal{N}_c$  as

$$\begin{aligned} (\mathcal{R}_c(u, v), \rho) &:= A\mathcal{N}_c(u, u; \rho) + B\mathcal{N}_c(u, v; \rho) + C\mathcal{N}_c(v, v; \rho), \\ (\mathcal{S}_c(u, v), \rho) &:= D\mathcal{N}_c(u, u; \rho) + E\mathcal{N}_c(u, v; \rho) + F\mathcal{N}_c(v, v; \rho), \end{aligned} \tag{2.17}$$

for  $\forall \rho \in V_h$ . Furthermore, the consistency of  $\mathcal{N}_c$  in (2.13) directly results in the consistency of  $\mathcal{R}_c$  and  $\mathcal{S}_c$ : for  $u, v \in H^1(I) \cap C_{per}(I)$  and  $\forall \rho \in V_h$ , i.e.,

$$\begin{aligned} (\mathcal{R}_c(u, v), \rho) &= (R(u, v)_x, \rho), \\ (\mathcal{S}_c(u, v), \rho) &= (S(u, v)_x, \rho). \end{aligned} \tag{2.18}$$

- **Dissipative-type notations and definitions.** We also introduce a dissipative-type numerical flux for the nonlinear terms  $R$  and  $S$  defined in (2.2) and (2.3) as follows

$$\widehat{\mathcal{R}}_d(u, v) = \{R(u, v)\} - \frac{\varepsilon}{2}[u], \tag{2.19}$$

$$\widehat{\mathcal{S}}_d(u, v) = \{S(u, v)\} - \frac{\varepsilon}{2}[v], \tag{2.20}$$

herein the positive parameter  $\varepsilon$  satisfies

$$\varepsilon \geq \varrho_0 \left( \frac{\partial(R, S)}{\partial(u, v)} \right), \tag{2.21}$$

and  $\varrho_0(\frac{\partial(R, S)}{\partial(u, v)})$  is the spectral radius of the Jacobian matrix of  $(R, S)^T$  over all  $u$  and  $v$ . Furthermore, some additional conditions for  $\varepsilon$  to ensure the stability of numerical scheme will be discussed in subsequent study.

We define the corresponding trilinear form  $\mathcal{N}_d$  as follows: for  $u, v, \rho \in H^1(\mathcal{T}_h)$ ,

$$\mathcal{N}_d(u, v; \rho) = - \sum_{j=1}^N (uv, \rho_x)_{I_j} - \sum_{j=1}^N (\{uv\}[\rho])_{j-\frac{1}{2}}. \tag{2.22}$$

In addition to the corresponding nonlinear operator  $\mathcal{N}_d : H^1(\mathcal{T}_h) \times H^1(\mathcal{T}_h) \rightarrow V_h$  in the sense of  $L^2[0, 1]$ -inner product: for  $\forall \rho \in V_h$ ,

$$(\mathcal{N}_d(u, v), \rho) = - \sum_{j=1}^N (uv, \rho_x)_{I_j} - \sum_{j=1}^N (\{uv\}[\rho])_{j-\frac{1}{2}}. \tag{2.23}$$

We list here some essential facts about this operator  $\mathcal{N}_d$ .

**Lemma 2.6** (The properties of  $\mathcal{N}_d$ ) *The trilinear form as defined in (2.22) satisfies*

1.  $\mathcal{N}_d$  is consistent in the sense that,

$$\mathcal{N}_d(u, v; \rho) = ((uv)_x, \rho), \text{ for } u, v \in H^1(I) \cap C_{per}(I), \quad \rho \in V_h. \tag{2.24}$$

2. For  $u, v \in H^1(\mathcal{T}_h)$ ,

$$\mathcal{N}_d(u, u; v) + 2\mathcal{N}_d(u, v; u) = -\frac{1}{2} \sum_{j=1}^N ([u][u][v])_{j-\frac{1}{2}}. \tag{2.25}$$

3. For  $u \in H^1(\mathcal{T}_h)$ ,

$$\mathcal{N}_d(u, u; u) = -\frac{1}{6} \sum_{j=1}^N ([u][u][u])_{j-\frac{1}{2}}. \tag{2.26}$$

**Proof** 1. For  $u, v \in H^1(I) \cap C_{per}(I)$ , the conclusion (2.24) is obtained by integration by parts, periodicity and continuity at each node.

2. Apply the periodic boundary condition and integration by parts to the definition of (2.22), then we get

$$\begin{aligned} & \mathcal{N}_d(u, u; v) + 2\mathcal{N}_d(u, v; u) \\ &= - \sum_{j=1}^N \left( 2(uv, u_x)_{I_j} + (uu, v_x)_{I_j} \right) - \sum_{j=1}^N \left( 2(\{uv\}[u])_{j-\frac{1}{2}} + (\{uu\}[v])_{j-\frac{1}{2}} \right) \\ &= \sum_{j=1}^N (\{uuv\} - 2\{uv\}[u] - \{uu\}[v])_{j-\frac{1}{2}} = \sum_{j=1}^N (2[u](\{u\}\{v\} - \{uv\}))_{j-\frac{1}{2}} \\ &= -\frac{1}{2} \sum_{j=1}^N ([u][u][v])_{j-\frac{1}{2}}. \end{aligned}$$

3. The result in (2.26) is a direct outcome when we replace  $v = u$  in (2.25) that

$$\mathcal{N}_d(u, u; u) + 2\mathcal{N}_d(u, u; u) = -\frac{1}{2} \sum_{j=1}^N ([u][u][u])_{j-\frac{1}{2}}.$$

□

**Remark 2.7** By some similar analysis, the consistency of  $\mathcal{N}_d$  directly deduces the consistency of the nonlinear terms: for  $u, v \in H^1(I) \cap C_{per}(I)$  and  $\forall \rho \in V_h$

$$\begin{aligned} (\mathcal{R}_d(u, v), \rho) &= (R(u, v)_x, \rho), \\ (\mathcal{S}_d(u, v), \rho) &= (S(u, v)_x, \rho), \end{aligned} \tag{2.27}$$

here the bilinear operator  $\mathcal{R}_d$  and  $\mathcal{S}_d$  are defined as

$$\begin{aligned} (\mathcal{R}_d(u, v), \rho) &= A\mathcal{N}_d(u, u; \rho) + B\mathcal{N}_d(u, v; \rho) + C\mathcal{N}_d(v, v; \rho) + \frac{\varepsilon}{2} \sum_{j=1}^N ([u][\rho])_{j-\frac{1}{2}}, \\ (\mathcal{S}_d(u, v), \rho) &= D\mathcal{N}_d(u, u; \rho) + E\mathcal{N}_d(u, v; \rho) + F\mathcal{N}_d(v, v; \rho) + \frac{\varepsilon}{2} \sum_{j=1}^N ([v][\rho])_{j-\frac{1}{2}}. \end{aligned} \tag{2.28}$$

The extra jumps  $[u]$  and  $[v]$  will vanish when  $u, v$  are periodic and continuous.

### 2.2.2 Properties to Linear Terms

Other than the notations and definitions for the nonlinear terms in the KdV-type system, in the future LDG schemes, we would like to define the useful bilinear forms  $\mathcal{D} : H^1(\mathcal{T}_h) \times H^1(\mathcal{T}_h) \rightarrow \mathbb{R}$  for linear terms: for  $w, \rho \in H^1(\mathcal{T}_h)$ ,

$$\mathcal{D}(w, \rho) = - \sum_{j=1}^N (w, \rho_x)_{I_j} - \sum_{j=1}^N (\widehat{w}[\rho])_{j-\frac{1}{2}}. \tag{2.29}$$

By the Riesz Representation Theorem, this bilinear form can be used to define the linear operator  $\mathcal{D} : H^1(\mathcal{T}_h) \rightarrow V_h$  with the following  $L^2[0, 1]$ -inner product: for  $\forall \rho \in V_h$ ,

$$(\mathcal{D}(w), \rho) = - \sum_{j=1}^N (w, \rho_x)_{I_j} - \sum_{j=1}^N (\widehat{w}[\rho])_{j-\frac{1}{2}}. \tag{2.30}$$

Furthermore, for different choices of the numerical flux of  $w$ , we use the specific notations  $\mathcal{D}^-$ ,  $\mathcal{D}^+$  and  $\mathcal{D}^*$  with  $\widehat{w}$  taking  $w^-$ ,  $w^+$  and  $\{w\}$ , respectively. Some properties of  $\mathcal{D}$  are displayed in the following Lemma.

**Lemma 2.8** (The properties of  $\mathcal{D}$ ) *The bilinear form  $\mathcal{D}$  defined in (2.30) satisfies*

1.  $\mathcal{D}$  is consistent in the sense that,

$$\mathcal{D}(u, \xi) = (u_x, \xi), \quad \text{for } u \in H^1(I) \cap C_{per}(I), \quad \xi \in V_h. \tag{2.31}$$

2. For  $\xi, \zeta \in H^1(\mathcal{T}_h)$ ,

$$\mathcal{D}^+(\xi, \zeta) + \mathcal{D}^-(\zeta, \xi) = 0, \tag{2.32}$$

$$\mathcal{D}^*(\xi, \zeta) + \mathcal{D}^*(\zeta, \xi) = 0. \tag{2.33}$$

3. For  $\xi \in H^1(\mathcal{T}_h)$ ,

$$\mathcal{D}^*(\xi, \xi) = 0, \tag{2.34}$$

$$\mathcal{D}^+(\xi, \xi) = - \sum_{j=1}^N \left( \frac{1}{2} [\xi]^2 \right)_{j-\frac{1}{2}}, \tag{2.35}$$

$$\mathcal{D}^-(\xi, \xi) = \sum_{j=1}^N \left( \frac{1}{2} [\xi]^2 \right)_{j-\frac{1}{2}}. \tag{2.36}$$

- Proof** 1. For  $u, v \in H^1(I) \cap C_{per}(I)$ , the consistency of  $\mathcal{D}$  can be obtained by integration by parts, periodicity and continuity at each node.
2. Apply integration by parts and periodicity to the definition of the linear form  $\mathcal{D}$ , then manipulate it as follows

$$\begin{aligned} & \mathcal{D}^+(\xi, \zeta) + \mathcal{D}^-(\zeta, \xi) \\ &= - \sum_{j=1}^N (\xi, \zeta_x)_{I_j} - \sum_{j=1}^N (\xi^+[\zeta])_{j-\frac{1}{2}} - \sum_{j=1}^N (\zeta, \xi_x)_{I_j} - \sum_{j=1}^N (\zeta^-[\xi])_{j-\frac{1}{2}} \\ &= \sum_{j=1}^N ((\xi \zeta)_{j-\frac{1}{2}}) - \sum_{j=1}^N (\xi^+[\zeta] + \zeta^-[\xi])_{j-\frac{1}{2}} \\ &= 0. \end{aligned}$$

The proof of the other equality is similar.

3. The result for  $\mathcal{D}^*(\xi, \xi)$  can be easily obtained by (2.33). And for  $\xi \in H^1(\mathcal{T}_h)$ , via integration by parts and periodicity, we have

$$\begin{aligned} \mathcal{D}^+(\xi, \xi) &= - \sum_{j=1}^N (\xi, \xi_x)_{I_j} - \sum_{j=1}^N (\xi^+[\xi])_{j-\frac{1}{2}} \\ &= \sum_{j=1}^N ((\xi \xi)_j - \xi^+[\xi])_{j-\frac{1}{2}} = - \sum_{j=1}^N \left( \frac{1}{2} [\xi]^2 \right)_{j-\frac{1}{2}}. \end{aligned}$$

Then equality (2.36) can be directly deduced by (2.32) and the above result. □

### 3 LDG Schemes for the KdV-Type System

We devote this section to the design of different LDG schemes for the KdV-type system (1.1) via choosing different numerical fluxes.

Rewrite the two equations in (1.1) into the following first-order systems

$$\begin{aligned} u_t + (p^{(u)})_x + R(u, v)_x &= 0, \\ p^{(u)} - (q^{(u)})_x &= 0, \\ q^{(u)} - u_x &= 0, \end{aligned} \tag{3.1}$$

and

$$\begin{aligned} v_t + (p^{(v)})_x + S(u, v)_x &= 0, \\ p^{(v)} - (q^{(v)})_x &= 0, \\ q^{(v)} - v_x &= 0. \end{aligned} \tag{3.2}$$

### 3.1 The Weak Formulation

We use the LDG method to approximate (3.1) and (3.2) as follow: For each  $j$ , find  $u_h, p_h^{(u)}, q_h^{(u)}, v_h, p_h^{(v)}, q_h^{(v)} \in V_h$  such that for all test functions  $\rho_1, \xi_1, \zeta_1, \rho_2, \xi_2, \zeta_2 \in V_h$ ,

$$\begin{aligned} & ((u_h)_t, \rho_1)_{I_j} - (p_h^{(u)}, (\rho_1)_x)_{I_j} + (\widehat{p}_h^{(u)} \rho_1^-)_{j+\frac{1}{2}} - (\widehat{p}_h^{(u)} \rho_1^+)_{j-\frac{1}{2}} \\ & - (R, (\rho_1)_x)_{I_j} + (\widehat{R} \rho_1^-)_{j+\frac{1}{2}} - (\widehat{R} \rho_1^+)_{j-\frac{1}{2}} = 0, \end{aligned} \tag{3.3}$$

$$(p_h^{(u)}, \xi_1)_{I_j} + (q_h^{(u)}, (\xi_1)_x)_{I_j} - (\widehat{q}_h^{(u)} \xi_1^-)_{j+\frac{1}{2}} + (\widehat{q}_h^{(u)} \xi_1^+)_{j-\frac{1}{2}} = 0, \tag{3.4}$$

$$(q_h^{(u)}, \zeta_1)_{I_j} + (u_h, (\zeta_1)_x)_{I_j} - (\widehat{u}_h \zeta_1^-)_{j+\frac{1}{2}} + (\widehat{u}_h \zeta_1^+)_{j-\frac{1}{2}} = 0, \tag{3.5}$$

and

$$\begin{aligned} & ((v_h)_t, \rho_2)_{I_j} - (p_h^{(v)}, (\rho_2)_x)_{I_j} + (\widehat{p}_h^{(v)} \rho_2^-)_{j+\frac{1}{2}} - (\widehat{p}_h^{(v)} \rho_2^+)_{j-\frac{1}{2}} \\ & - (S, (\rho_2)_x)_{I_j} + (\widehat{S} \rho_2^-)_{j+\frac{1}{2}} - (\widehat{S} \rho_2^+)_{j-\frac{1}{2}} = 0, \end{aligned} \tag{3.6}$$

$$(p_h^{(v)}, \xi_2)_{I_j} + (q_h^{(v)}, (\xi_2)_x)_{I_j} - (\widehat{q}_h^{(v)} \xi_2^-)_{j+\frac{1}{2}} + (\widehat{q}_h^{(v)} \xi_2^+)_{j-\frac{1}{2}} = 0, \tag{3.7}$$

$$(q_h^{(v)}, \zeta_2)_{I_j} + (v_h, (\zeta_2)_x)_{I_j} - (\widehat{v}_h \zeta_2^-)_{j+\frac{1}{2}} + (\widehat{v}_h \zeta_2^+)_{j-\frac{1}{2}} = 0. \tag{3.8}$$

Here, the ‘‘hat’’ terms are numerical fluxes as described before, and  $(\cdot, \cdot)_{I_j}$  denotes the  $L^2$  inner product over the cell  $I_j$ .

### 3.2 The Numerical Fluxes

We remark that different choices of the numerical fluxes  $\widehat{R}, \widehat{S}, \widehat{p}_h^{(\chi)}, \widehat{q}_h^{(\chi)}$  and  $\widehat{\chi}_h$  (here  $\chi$  can be  $u$  or  $v$ ) would result in different numerical LDG schemes for the KdV-type system (1.1). Herein, we list the choices of the numerical fluxes as follows:

1. The conservative fluxes for  $p_h^{(\chi)}, q_h^{(\chi)}$  and  $\chi_h$

$$\widehat{p}_h^{(\chi)} = \{p^{(\chi)}\}, \quad \widehat{q}_h^{(\chi)} = \{q_h^{(\chi)}\}, \quad \widehat{\chi}_h = \{\chi_h\}. \tag{3.9}$$

2. The dissipative fluxes for  $p_h^{(\chi)}, q_h^{(\chi)}$  and  $\chi_h$

$$\widehat{p}_h^{(\chi)} = (p_h^{(\chi)})^+, \quad \widehat{q}_h^{(\chi)} = (q_h^{(\chi)})^+, \quad \widehat{\chi}_h = \chi_h^-. \tag{3.10}$$

3. The conservative fluxes for  $R$  and  $S$  as described in (2.5) and (2.6)

$$\begin{aligned} \widehat{R}_c(u_h, v_h) &= A \widehat{f}(u_h, u_h) + B \widehat{f}(u_h, v_h) + C \widehat{f}(v_h, v_h), \\ \widehat{S}_c(u_h, v_h) &= D \widehat{f}(u_h, u_h) + E \widehat{f}(u_h, v_h) + F \widehat{f}(v_h, v_h). \end{aligned} \tag{3.11}$$

4. The dissipative fluxes for  $R$  and  $S$  as defined in (2.19) and (2.20)

$$\begin{aligned} \widehat{R}_d(u_h, v_h) &= \{R(u_h, v_h)\} - \frac{\varepsilon}{2}[u_h], \\ \widehat{S}_d(u_h, v_h) &= \{S(u_h, v_h)\} - \frac{\varepsilon}{2}[v_h]. \end{aligned} \tag{3.12}$$

**Table 1** Four LDG schemes for KdV-type system

	Conservative ( $\widehat{S}_c, \widehat{R}_c$ ) in (3.11)	Dissipative ( $\widehat{S}_d, \widehat{R}_d$ ) in (3.12)
Conservative ( $\widehat{p}_h^{(x)}, \widehat{q}_h^{(x)}, \widehat{\chi}_h$ ) in (3.9)	$C_l$ – $C_n$ scheme	$C_l$ – $D_n$ scheme
Dissipative ( $\widehat{p}_h^{(x)}, \widehat{q}_h^{(x)}, \widehat{\chi}_h$ ) in (3.10)	$D_l$ – $C_n$ scheme	$D_l$ – $D_n$ scheme

The so-called “conservative” and “dissipative” labels in above statements will be specified in the next section. These four choices lead to one conservative LDG scheme with numerical fluxes (3.9) and (3.11), as well as three dissipative schemes for the KdV-type system. We display all four schemes in Table 1.

**Remark 3.1** We remark that the choices of numerical fluxes of  $\widehat{p}_h^{(x)}$  and  $\widehat{\chi}_h$  in (3.9) and (3.10) are not unique for they just need to follow some cardinal rule:  $\widehat{p}_h^{(x)}$  and  $\widehat{\chi}_h$  must be taken from opposite sides. And here we list a sequence of possible choices of the numerical fluxes

$$\begin{aligned} \widehat{p}_h^{(x)} &= \{p_h^{(x)}\} + \theta[p_h^{(x)}], \\ \widehat{\chi}_h &= \{\chi_h\} - \theta[\chi_h], \end{aligned}$$

where  $\theta$  is a constant in  $[-\frac{1}{2}, \frac{1}{2}]$ . Particularly,  $\theta$  taking  $\pm\frac{1}{2}$  leads to the alternating fluxes and  $\theta = 0$  to the central fluxes. In this paper, we will only focus our work on the fluxes presented in (3.9) and (3.10) and the analogous analysis about the other fluxes can be easy obtained by results of these two particular cases.

### 4 Conservative Properties and Stability Analysis

In this section, we turn to discuss and analyze the stability of the LDG schemes presented in previous section. According to the discrete version of energy  $\mathcal{H}$  defined in (1.3), we say that the  $\mathcal{H}$ -stability holds when

$$\mathcal{H}(u_h, v_h) = \int_I (au_h^2 + bu_hv_h + cv_h^2)dx \leq 0, \quad \text{for } u_h, v_h \in V_h,$$

in particular, if the equality holds, we called it as  $\mathcal{H}$ -conservation. Besides, the corresponding adjective expressions, such as “ $\mathcal{H}$ -dissipative” and “ $\mathcal{H}$ -conservative”, are also used in this paper. We will see in next subsection that when the conservative numerical fluxes (3.9) and (3.11) are both taking, the  $\mathcal{H}$ -conservation will hold; or else only the  $\mathcal{H}$ -dissipative property can be obtained.

#### 4.1 Main Results About the Stability Analysis

**Theorem 4.1** Assume that  $a, b, c$  are solutions of the system (1.4) and satisfy condition (1.5). Let  $u_h, v_h \in V_h$  be the numerical solutions of the LDG schemes (3.3)–(3.8) equipped with numerical fluxes aforementioned in Table 1, then we have the following results.

- ( $C_l$ – $C_n$  scheme) The  $C_l$ – $C_n$  scheme is  $\mathcal{H}$ -conservative,

$$\frac{d}{dt} \mathcal{H}(u_h, v_h) = 0. \tag{4.1}$$

- ( $C_l-D_n$  scheme) The  $C_l-D_n$  scheme possesses the  $\mathcal{H}$ -stability,

$$\frac{d}{dt} \mathcal{H}(u_h, v_h) \leq 0. \tag{4.2}$$

- ( $D_l-C_n, D_l-D_n$  schemes) Further assume that the parameters in condition (1.5) are nonnegative, i.e.,  $a, b, c \geq 0$ , then the other two dissipative schemes,  $D_l-C_n$  and  $D_l-D_n$ , admit the  $\mathcal{H}$ -stability

$$\frac{d}{dt} \mathcal{H}(u_h, v_h) \leq 0, \tag{4.3}$$

if the positive constant  $\varepsilon$  in  $\widehat{R}_d$  and  $\widehat{S}_d$  satisfies

$$\varepsilon \geq \max \left( \frac{1}{\alpha} |\Lambda_1|, \frac{1}{\alpha} |\Lambda_2|, \varrho_0 \left( \frac{\partial(R, S)}{\partial(u, v)} \right) \right), \tag{4.4}$$

where  $\alpha$  is some positive number generated by condition (1.5) such that

$$\alpha(\|u\|^2 + \|v\|^2) \leq \mathcal{H}(u, v) = au^2 + buv + cv^2$$

and  $\Lambda_1, \Lambda_2$  denote

$$\begin{aligned} \Lambda_1 &= \frac{1}{3}(2aA + bD)\|u\|_\infty + (2cD + bA)\|v\|_\infty, \\ \Lambda_2 &= \frac{1}{3}(bC + 2cF)\|v\|_\infty + (2aC + bF)\|u\|_\infty. \end{aligned} \tag{4.5}$$

**Remark 4.2** We remark that the  $\mathcal{H}$ -stability of the  $D_l-C_n$  scheme and  $D_l-D_n$  scheme are restricted by the values of  $a, b$  and  $c$ , since the stability analysis for linear terms hold with  $a, b, c \geq 0$ . Such extra assumption indicates that only a part of  $\mathcal{H}$  quantities are proven stable by our method, yet it is not to say that the remaining quantities perform badly in these LDG schemes. In the future section of numerical experiments, we choose some examples which are not satisfied with condition  $a, b, c \geq 0$ , but the numerical results still perform well therein.

**Remark 4.3** Taking into consideration of the condition (1.5), there exists a positive constant  $\alpha$  such that

$$\alpha \int_0^1 (u_h^2 + v_h^2) dx \leq \mathcal{H}(u_h, v_h), \tag{4.6}$$

and this indicates the global boundary for  $\|u_h\|$  and  $\|v_h\|$ .

### 4.2 Proof of the Main Results

We first consider Eqs. (3.3) and (3.6) in two systems. Sum over all cells and notice the periodic condition, then (3.3) and (3.6) become

$$\begin{aligned} & \sum_{j=1}^N ((u_h)_t, \rho_1)_{I_j} - \sum_{j=1}^N \left( \left( p_h^{(u)}(\rho_1)_x \right)_{I_j} + \left( \widehat{p}_h^{(u)}[\rho_1] \right)_{j-\frac{1}{2}} \right) \\ & - \sum_{j=1}^N \left( (R, (\rho_1)_x)_{I_j} + (\widehat{R}[\rho_1])_{j-\frac{1}{2}} \right) = 0, \end{aligned} \tag{4.7}$$

$$\begin{aligned} & \sum_{j=1}^N ((v_h)_t, \rho_2)_{I_j} - \sum_{j=1}^N \left( (p_h^{(v)}(\rho_2)_x)_{I_j} + (\widehat{p}_h^{(v)}[\rho_2])_{j-\frac{1}{2}} \right) \\ & - \sum_{j=1}^N \left( (S, (\rho_2)_x)_{I_j} + (\widehat{S}[\rho_2])_{j-\frac{1}{2}} \right) = 0, \end{aligned} \tag{4.8}$$

here  $\widehat{p}_h^{(u)}, \widehat{p}_h^{(v)}, \widehat{R}$  and  $\widehat{S}$  are generalized notations with different choices in different schemes aforementioned. By virtue of the linear operator  $\mathcal{D}$  and nonlinear operators  $\mathcal{B}$  and  $\mathcal{S}$ , we can concisely rewrite (4.7) and (4.8) as follows

$$(u_h)_t + \mathcal{D}(p_h^{(u)}) + \mathcal{B}(u_h, v_h) = 0, \tag{4.9}$$

$$(v_h)_t + \mathcal{D}(p_h^{(v)}) + \mathcal{S}(u_h, v_h) = 0. \tag{4.10}$$

Multiplying (4.9) and (4.10) by  $2au_h + bv_h$  and  $bu_h + 2cv_h$  respectively, then integrating and summing up, we get the following important equation

$$\frac{d}{dt} \mathcal{H}(u_h, v_h) + \mathcal{J}(u_h, v_h; p_h^{(u)}, p_h^{(v)}) + \mathcal{I}(u_h, v_h) = 0, \tag{4.11}$$

where  $\mathcal{J}(u_h, v_h; p_h^{(u)}, p_h^{(v)})$  denotes

$$\begin{aligned} \mathcal{J}(u_h, v_h; p_h^{(u)}, p_h^{(v)}) &= 2a\mathcal{D}(p_h^{(u)}, u_h) + b(\mathcal{D}(p_h^{(u)}, v_h) \\ & \quad + \mathcal{D}(p_h^{(v)}, u_h)) + 2c\mathcal{D}(p_h^{(v)}, v_h), \end{aligned} \tag{4.12}$$

and  $\mathcal{I}(u_h, v_h)$  is defined as

$$\mathcal{I}(u_h, v_h) = (\mathcal{B}(u_h, v_h), 2au_h + bv_h) + (\mathcal{S}(u_h, v_h), bu_h + 2cv_h). \tag{4.13}$$

In the following discussion, for different schemes, we will further denote  $\mathcal{J}_c$  and  $\mathcal{J}_d$  according to  $\mathcal{D}$  in (4.12) being  $\mathcal{D}^*$  and  $\mathcal{D}^+$ , respectively,

$$\begin{aligned} \mathcal{J}_c(u_h, v_h; p_h^{(u)}, p_h^{(v)}) &= 2a\mathcal{D}^*(p_h^{(u)}, u_h) + b(\mathcal{D}^*(p_h^{(u)}, v_h) \\ & \quad + \mathcal{D}^*(p_h^{(v)}, u_h)) + 2c\mathcal{D}^*(p_h^{(v)}, v_h), \\ \mathcal{J}_d(u_h, v_h; p_h^{(u)}, p_h^{(v)}) &= 2a\mathcal{D}^+(p_h^{(u)}, u_h) + b(\mathcal{D}^+(p_h^{(u)}, v_h) \\ & \quad + \mathcal{D}^+(p_h^{(v)}, u_h)) + 2c\mathcal{D}^+(p_h^{(v)}, v_h). \end{aligned}$$

Similarly, we use  $\mathcal{I}_c$  and  $\mathcal{I}_d$  to denote the different cases of (4.13) according to the nonlinear fluxes pair  $(\widehat{R}, \widehat{S})$  respectively taking the conservative case  $(\widehat{R}_c, \widehat{S}_c)$  in (3.11) and the dissipative one  $(\widehat{R}_d, \widehat{S}_d)$  in (3.12), namely

$$\begin{aligned} \mathcal{I}_c(u_h, v_h) &= (\mathcal{B}_c(u_h, v_h), 2au_h + bv_h) + (\mathcal{S}_c(v_h, v_h), bu_h + 2cv_h), \\ \mathcal{I}_d(u_h, v_h) &= (\mathcal{B}_d(u_h, v_h), 2au_h + bv_h) + (\mathcal{S}_d(u_h, v_h), bu_h + 2cv_h). \end{aligned}$$

We first give the following lemma for nonlinear quantity  $\mathcal{I}$ .

**Lemma 4.4** (The properties of  $\mathcal{I}$ ) *Let  $a, b, c$  be solutions of the system (1.4) and satisfy (1.5). Then for  $u_h, v_h \in V_h$ , there hold the following facts for quantities  $\mathcal{I}_c$  and  $\mathcal{I}_d$*

- Take  $\widehat{R} = \widehat{R}_c, \widehat{S} = \widehat{S}_c$ , then the following equality holds

$$\mathcal{I}_c(u_h, v_h) = 0. \tag{4.14}$$

- Take  $\widehat{R} = \widehat{R}_d$ ,  $\widehat{S} = \widehat{S}_d$ , and further suppose the parameter  $\varepsilon$  in  $\widehat{R}_d$  and  $\widehat{S}_d$  satisfies the condition mentioned in (4.4), then there holds

$$\mathcal{I}_d(u_h, v_h) \geq 0. \tag{4.15}$$

**Proof** The detailed proofs are given in Appendix A. □

Now we turn to analyze the quantities  $\mathcal{J}_c$  and  $\mathcal{J}_d$  in the following lemma.

**Lemma 4.5** (The properties of  $\mathcal{J}$ ) *Let  $a, b, c$  be solutions of the system (1.4) and satisfy condition (1.5). For the quantities  $\mathcal{J}_c$  and  $\mathcal{J}_d$  generated by the linear terms in the system, we have the following (in)equalities*

- Take the numerical fluxes of the linear terms as in (3.9), then there holds the following equality for  $\mathcal{J}_c$

$$\mathcal{J}_c(u_h, v_h; p_h^{(u)}, p_h^{(v)}) = 0. \tag{4.16}$$

- Take the numerical fluxes of the linear terms as in (3.10) and further assume the parameter  $b \geq 0$ , then there holds the following inequality for  $\mathcal{J}_d$

$$\mathcal{J}_d(u_h, v_h; p_h^{(u)}, p_h^{(v)}) \geq 0. \tag{4.17}$$

**Proof** The detailed proofs are given in Appendix B. □

We further apply the results of Lemmas 4.4 and 4.5 and finally obtain the desired results as follows

- ( $\mathbf{C}_l$ - $\mathbf{C}_n$  scheme)

$$0 = \frac{d}{dt} \mathcal{H}(u_h, v_h) + \mathcal{J}_c(u_h, v_h; p_h^{(u)}, p_h^{(v)}) + \mathcal{I}_c(u_h, v_h) = \frac{d}{dt} \mathcal{H}(u_h, v_h). \tag{4.18}$$

- ( $\mathbf{D}_l$ - $\mathbf{C}_n$  scheme)

$$0 = \frac{d}{dt} \mathcal{H}(u_h, v_h) + \mathcal{J}_d(u_h, v_h; p_h^{(u)}, p_h^{(v)}) + \mathcal{I}_c(u_h, v_h) \geq \frac{d}{dt} \mathcal{H}(u_h, v_h). \tag{4.19}$$

- ( $\mathbf{C}_l$ - $\mathbf{D}_n$  scheme)

$$0 = \frac{d}{dt} \mathcal{H}(u_h, v_h) + \mathcal{J}_c(u_h, v_h; p_h^{(u)}, p_h^{(v)}) + \mathcal{I}_d(u_h, v_h) \geq \frac{d}{dt} \mathcal{H}(u_h, v_h). \tag{4.20}$$

- ( $\mathbf{D}_l$ - $\mathbf{D}_n$  scheme)

$$0 = \frac{d}{dt} \mathcal{H}(u_h, v_h) + \mathcal{J}_d(u_h, v_h; p_h^{(u)}, p_h^{(v)}) + \mathcal{I}_d(u_h, v_h) \geq \frac{d}{dt} \mathcal{H}(u_h, v_h). \tag{4.21}$$

Now we have completed the proofs of the main results about the conservative and dissipative properties for our designed schemes.

## 5 Error Estimates

In what follows, we derive error estimates for the  $\mathbf{D}_l$ - $\mathbf{C}_n$  scheme and  $\mathbf{D}_l$ - $\mathbf{D}_n$  scheme with both taking the dissipative numerical fluxes for the linear terms in the KdV-type system (1.1). For the LDG methods to nonlinear KdV equations, we know that there exists some obstacles in handling the error estimates for the linear terms choosing  $\widehat{q}_h^{(x)} = \{q_h^{(x)}\}$ . For example,

authors in [16] say that they only obtain the best  $(k - \frac{1}{2})$  order of accuracy after trying various different approaches to derive a priori error estimates for the conservative LDG method to the gKdV equation. For this reason, we just choose the dissipative flux  $\widehat{q}_h^{(x)} = (q_h^{(x)})^+$  in this section and focus our attention on the performance of two different nonlinear numerical fluxes, (3.11) and (3.12).

Our ideas of handling the error estimates for linear terms of the KdV system are guided by the LDG method to nonlinear KdV equation in [22]; the strategies for nonlinear terms are inspired by the continuous Galerkin method to the KdV-type system in [5] and the DG method to symmetrizable systems of conservation laws in [30].

The framework of this section is designed as follows: we supplement some useful notations and auxiliary tools for the following error estimates in Sect. 5.1; then we put forward the main error estimate results for both two schemes in Sect. 5.2 in advance; after that we give the analysis for the main results by separating the proof into 2 parts: Sect. 5.3 for generating the error equation, and Sect. 5.4 about error estimate for each term of the error equation.

### 5.1 Notations and Auxiliary Results

In this part, we introduce some notations and assumptions to be used and some auxiliary results to be cited later in this paper. Some projections are introduced and the corresponding interpolation and inverse properties for the finite element spaces are presented.

#### 5.1.1 Notations and Assumptions

We will denote by  $C$  and  $C_*$  positive constants independent of  $h$  and  $N$ , which may depend on the solutions of the KdV-type system considered in this paper. Especially,  $C_*$  used to emphasize the nonlinearity of fluxes  $F(u, v)$  and  $G(u, v)$  depends on the maximum of second derivatives of  $F$  and/or  $G$ . These constants may have a different value in each occurrence for the sake of facility. In this part, the exact solutions of the problem to be considered are assumed to be smooth equipped with the periodic or compactly supported boundary conditions. The time evolution about the problem is also bounded as  $0 \leq t \leq T$  for a fixed  $T$ . As a result, the exact solutions are bounded too.

#### 5.1.2 E-flux and an Important Matrix Related to the Numerical Flux

- **The E-flux.** Let  $\mathbf{p} = (u, v)^T$ . We say that a system with the nonlinear terms  $P(u, v)$  and  $Q(u, v)$  is symmetric if  $\mathcal{B} := (P, Q)^T$  satisfies that the Jacobian matrix  $\mathbb{J}_{\mathcal{B}} = \frac{\partial(P, Q)}{\partial(u, v)}$  is a symmetric matrix. For a symmetric system of conservation laws, the numerical flux  $\widehat{\mathcal{B}} := \widehat{\mathcal{B}}(\mathbf{p}^-, \mathbf{p}^+)$  has been considered as an E-flux in [14] and [30] (therein they called it a generalized E-flux on account of handling their targeted symmetrizable system) if it is Lipschitz continuous and the following inequality holds

$$(\mathcal{B}(r_i) - \widehat{\mathcal{B}}(\mathbf{p}^-, \mathbf{p}^+))(\mathbf{p}^+ - \mathbf{p}^-)^T \geq 0, \quad i = 1, 2, 3, \tag{5.1}$$

where  $r_i = \mathbf{p}^-, \{\mathbf{p}\}$  and  $\mathbf{p}^+$ .

Many numerical fluxes can be verified easily to be (generalized) E-fluxes: for example, the Roe linearization flux function [19], with or without Harten’s entropy fix [13], and the global (local) Lax–Friedrichs flux which has been shown to be in [14] and detailedly discussed in [18].

Last but not least, we must remark that our KdV-type system (1.1) with  $\mathcal{K} = (R, S)^T$  is not a symmetric system since  $\mathbb{J}_{\mathcal{K}}$  being not symmetric, yet we can use some extra conditions to generate some symmetric form  $\mathcal{B} = (P, Q)^T$ . Such discussion will be put in Sect. 5.4.

- **An important matrix related to the numerical flux.** The symmetric system along with the E-flux property guides us to introduce an important matrix in measuring the amount of numerical viscosity presented in [30]. Comparing to the original description about the symmetrizable system in [30], we only list herein the simplified version for the symmetric system in the following proposition.

**Proposition 5.1** *Assume that the numerical flux  $\widehat{\mathcal{B}} = \widehat{\mathcal{B}}(\mathbf{p}^-, \mathbf{p}^+)$  satisfies the generalized E-flux property (5.1) and consistent with the flux  $\mathcal{B}(\mathbf{p})$ . Define the matrix on each element interface*

$$\mathcal{A}(\widehat{\mathcal{B}}; \mathbf{p}) \equiv \mathcal{A}(\widehat{\mathcal{B}}; \mathbf{p}^-, \mathbf{p}^+) := \begin{cases} \frac{1}{6}\mathcal{A}_1 + \frac{2}{3}\mathcal{A}_2 + \frac{1}{6}\mathcal{A}_3, & \text{if } [\mathbf{p}] \neq 0, \\ |\mathbb{J}_{\mathcal{B}}(\{\mathbf{p}\})|, & \text{if } [\mathbf{p}] = 0, \end{cases} \tag{5.2}$$

where

$$\mathcal{A}_i = \frac{(\mathcal{B}(\mathbf{r}_i) - \widehat{\mathcal{B}}(\mathbf{p}))[\mathbf{p}]^T}{[\mathbf{p}]^T [\mathbf{p}]}, \quad i = 1, 2, 3, \tag{5.3}$$

with  $\mathbf{r}_i = \mathbf{p}^-, \{\mathbf{p}\}, \mathbf{p}^+$  as defined in (5.1). Then for any  $\mathbf{p} \in \mathbb{R}^2$ , the spectrum of  $\mathcal{A}(\widehat{\mathcal{B}}; \mathbf{p})$  is bounded and  $[\mathbf{p}]^T \mathcal{A}(\widehat{\mathcal{B}}; \mathbf{p})[\mathbf{p}] \geq 0$ ; what's more

$$\frac{1}{3}[\mathbf{p}]^T |\mathbb{J}_{\mathcal{B}}(\{\mathbf{p}\})|[\mathbf{p}] \leq [\mathbf{p}]^T \mathcal{A}(\widehat{\mathcal{B}}; \mathbf{p})[\mathbf{p}] + C_* \|\mathbf{p}\|^3, \tag{5.4}$$

where the positive constant  $C_*$  depends only on the nonlinearity of the flux  $\mathcal{B}$ , and  $\|\mathbf{p}\|$  is the length of the vector  $[\mathbf{p}]$ .

In our following discussion, some convenient notations for  $\mathcal{A}(\widehat{\mathcal{B}}; \mathbf{p})$  will be adopted when the intent is clear from the context, i.e.

$$A(\mathbf{p}) = \sum_{j=1}^N [\mathbf{p}]_{j-\frac{1}{2}}^T \mathcal{A}(\widehat{\mathcal{B}}; \mathbf{p})_{j-\frac{1}{2}} [\mathbf{p}]_{j-\frac{1}{2}}.$$

### 5.1.3 Projections and Interpolation Properties

In the following, we will introduce the standard  $L^2$ -projection of a continuous function  $\omega$  with  $k + 1$  order bounded derivatives into the finite element space  $V_h$ , denoted by  $\mathcal{P}$ ; i.e., for each  $j$ ,

$$\int_{I_j} (\mathcal{P}\omega(x) - \omega(x))v(x)dx = 0, \quad \text{for } \forall v \in P^k(I_j), \tag{5.5}$$

and the special projection  $\mathcal{P}^\pm$  into  $V_h$ , satisfying that: for each  $j$  and  $\forall v \in P^{k-1}(I_j)$ ,

$$\int_{I_j} (\mathcal{P}^+\omega(x) - \omega(x))v(x)dx = 0, \quad \text{and } \mathcal{P}^+\omega(x_{j-\frac{1}{2}}^+) = \omega(x_{j-\frac{1}{2}}), \tag{5.6}$$

$$\int_{I_j} (\mathcal{P}^-\omega(x) - \omega(x))v(x)dx = 0, \quad \text{and } \mathcal{P}^-\omega(x_{j+\frac{1}{2}}^-) = \omega(x_{j+\frac{1}{2}}). \tag{5.7}$$

For both projections mentioned above, authors in [29] generalized the following results from [9] as follows

$$\|\omega^e\| + h\|\omega^e\|_\infty + h^{\frac{1}{2}}\|\omega^e\|_{\Gamma_h} \leq Ch^{k+1}, \tag{5.8}$$

where  $\omega^e = \mathcal{P}\omega - \omega$ ,  $\omega^e = \mathcal{P}^+\omega - \omega$  or  $\omega^e = \mathcal{P}^-\omega - \omega$ . The positive constant C depends only on  $\omega$ , namely it is independent of  $h$ .  $\Gamma_h$  denotes the set of boundary points of all cells  $I_j$  belonging to the mesh grid, and the norm

$$\|u\|_{\Gamma_h} = \sqrt{\frac{1}{N} \sum_{j=1}^N \|u\|_{L^2(\partial I_j)}^2}.$$

### 5.1.4 Inverse Properties

We show several inverse properties of space  $V_h$  which will be utilized in the following error estimates. For any  $\omega_h \in V_h$ , there exists a positive constant C independent of  $\omega_h$  and  $h$ , such that

$$(i) \|\nabla\omega_h\| \leq Ch^{-1}\|\omega_h\|, \quad (ii) \|\omega_h\|_{\Gamma_h} \leq Ch^{-\frac{1}{2}}\|\omega_h\|, \quad (iii) \|\omega_h\|_\infty \leq Ch^{-\frac{1}{2}}\|\omega_h\|. \tag{5.9}$$

## 5.2 The Main Error Estimate Results

**Theorem 5.2** *Assume that  $a, b, c$  are solutions of the system (1.4) satisfying condition (1.5). Let  $u$  and  $v$  be the exact solutions of the KdV-type system (1.1) which are periodic and smooth enough with bounded derivatives. Let  $u_h, v_h \in V_h$  be the numerical solutions of the semi-discrete LDG schemes (3.3)–(3.8) equipped with numerical fluxes (3.10) for the linear terms and (3.11) or (3.12) for the nonlinear terms. Denote the corresponding numerical errors by  $e_u = u - u_h$  and  $e_v = v - v_h$ . For a regular partition of  $I = [0, 1]$  with  $N$  cells, we assume the finite element spaces  $V_h$  defined in (2.1) with discontinuous, piecewise polynomials of degree less than or equal to  $k$ . For sufficiently small  $h$  and assuming that  $\|u_h(0) - u(0)\| = O(h^{k+1})$  and  $\|v_h(0) - v(0)\| = O(h^{k+1})$ , the following error estimates hold*

- The numerical solutions  $u_h$  and  $v_h$  of the  $D_l$ - $C_n$  scheme equipped with the numerical fluxes (3.10) and (3.11) satisfy

$$\|u - u_h\|^2 + \|v - v_h\|^2 \leq Ch^{2k}. \tag{5.10}$$

- The numerical solutions  $u_h$  and  $v_h$  of the  $D_l$ - $D_n$  scheme equipped with the numerical fluxes (3.10) and (3.12) satisfy

$$\|u - u_h\|^2 + \|v - v_h\|^2 \leq Ch^{2k+1}. \tag{5.11}$$

Here the constant C depends on the terminal time  $T, k, \|u\|_\infty, \|v\|_\infty, \|u\|_{k+1}$  and  $\|v\|_{k+1}$ . The notation  $\|\cdot\|_{k+1}$  is the maximum over  $0 \leq t \leq T$  of the broken Sobolev  $(k + 1)$  norm in space.

## 5.3 The Error Equations and Energy Equality

We choose the projections as follows

$$s^{(x)} = \chi_h - \mathcal{P}^-\chi, \quad \eta^{(x)} = \chi - \mathcal{P}^-\chi,$$

$$\begin{aligned} w^{(\chi)} &= p_h^{(\chi)} - \mathcal{P}p^{(\chi)}, & \theta^{(\chi)} &= p^{(\chi)} - \mathcal{P}p^{(\chi)}, \\ y^{(\chi)} &= q_h^{(\chi)} - \mathcal{P}q^{(\chi)}, & \gamma^{(\chi)} &= q^{(\chi)} - \mathcal{P}q^{(\chi)}, \end{aligned} \tag{5.12}$$

where  $\chi$  can be  $u$  or  $v$ . Let  $u, v, p^{(u)}, p^{(v)}, q^{(u)}$  and  $q^{(v)}$  be periodic and sufficiently smooth solutions of the systems (3.1) and (3.2), and take account of the consistency of  $\mathcal{R}, \mathcal{S}, \mathcal{D}$  in (2.18), (2.27) and (2.31), then these exact solutions also satisfy the LDG schemes (3.3)–(3.5) and (3.6)–(3.8). We obtain the error equations in the distributional sense

$$s_t^{(u)} + \mathcal{D}^+(w^{(u)}) + \mathcal{R}(u_h, v_h) = \eta_t^{(u)} + \mathcal{D}^+(\theta^{(u)}) + \mathcal{R}(u, v), \tag{5.13}$$

$$w^{(u)} - \mathcal{D}^+(y^{(u)}) = \theta^{(u)} - \mathcal{D}^+(\gamma^{(u)}), \tag{5.14}$$

$$y^{(u)} - \mathcal{D}^-(s^{(u)}) = \gamma^{(u)} - \mathcal{D}^-(\eta^{(u)}), \tag{5.15}$$

and

$$s_t^{(v)} + \mathcal{D}^+(w^{(v)}) + \mathcal{S}(u_h, v_h) = \eta_t^{(v)} + \mathcal{D}^+(\theta^{(v)}) + \mathcal{S}(u, v), \tag{5.16}$$

$$w^{(v)} - \mathcal{D}^+(y^{(v)}) = \theta^{(v)} - \mathcal{D}^+(\gamma^{(v)}), \tag{5.17}$$

$$y^{(v)} - \mathcal{D}^-(s^{(v)}) = \gamma^{(v)} - \mathcal{D}^-(\eta^{(v)}), \tag{5.18}$$

here  $\mathcal{R}$  can be  $\mathcal{R}_c$  or  $\mathcal{R}_d$  and  $\mathcal{S}$  can be  $\mathcal{S}_c$  or  $\mathcal{S}_d$ .

The general  $L^2$ -projection  $\mathcal{P}$  have the property such that  $\theta^{(\chi)}$  and  $\gamma^{(\chi)}$  are orthogonal to  $V_h$ , and the special projection  $\mathcal{P}^-$  makes  $\eta^{(\chi)}$  locally orthogonal to all polynomials of degree up to  $k - 1$ . We list such useful facts as follows

- For  $\forall \phi \in V_h$ ,

$$\sum_{j=1}^N \left( (\theta^{(\chi)}), \phi \right)_{I_j} = 0, \quad \sum_{j=1}^N \left( (\gamma^{(\chi)}), \phi \right)_{I_j} = 0. \tag{5.19}$$

- For the bilinear form  $\mathcal{D}$  and  $\forall \phi \in V_h$ ,

$$\mathcal{D}^-(\eta^{(\chi)}, \phi) = - \sum_{j=1}^N \left( \eta^{(\chi)}, \phi_x \right)_{I_j} - \sum_{j=1}^N \left( (\eta^{(\chi)})^- [\phi] \right)_{j-\frac{1}{2}} = 0, \tag{5.20}$$

$$\mathcal{D}^+(\theta^{(\chi)}, \phi) = - \sum_{j=1}^N \left( \theta^{(\chi)}, \phi_x \right)_{I_j} - \sum_{j=1}^N \left( (\theta^{(\chi)})^+ [\phi] \right)_{j-\frac{1}{2}} = - \sum_{j=1}^N \left( (\theta^{(\chi)})^+ [\phi] \right)_{j-\frac{1}{2}}, \tag{5.21}$$

$$\mathcal{D}^+(\gamma^{(\chi)}, \phi) = - \sum_{j=1}^N \left( \gamma^{(\chi)}, \phi_x \right)_{I_j} - \sum_{j=1}^N \left( (\gamma^{(\chi)})^+ [\phi] \right)_{j-\frac{1}{2}} = - \sum_{j=1}^N \left( (\gamma^{(\chi)})^+ [\phi] \right)_{j-\frac{1}{2}}. \tag{5.22}$$

Now multiplying (5.13) by  $2as^{(u)} + bs^{(v)}$  and integrating, similarly (5.16) with  $bs^{(u)} + 2cs^{(v)}$ , then summing up, we obtain

$$\begin{aligned} & \frac{d}{dt} \mathcal{H}(s^{(u)}, s^{(v)}) + \left( 2a\mathcal{D}^+(w^{(u)}, s^{(u)}) + b\mathcal{D}^+(w^{(u)}, s^{(v)}) + b\mathcal{D}^+(w^{(v)}, s^{(u)}) + 2c\mathcal{D}^+(w^{(v)}, s^{(v)}) \right) \\ &= \sum_{j=1}^N \left( 2a \left( \eta_t^{(u)}, s^{(u)} \right)_{I_j} + b \left( \eta_t^{(u)}, s^{(v)} \right)_{I_j} + b \left( \eta_t^{(v)}, s^{(u)} \right)_{I_j} + 2c \left( \eta_t^{(v)}, s^{(v)} \right)_{I_j} \right) \end{aligned}$$

$$\begin{aligned}
 & - \left( 2a\mathcal{D}^+(\theta^{(u)}, s^{(u)}) + b\mathcal{D}^+(\theta^{(u)}, s^{(v)}) + b\mathcal{D}^+(\theta^{(v)}, s^{(u)}) + 2c\mathcal{D}^+(\theta^{(v)}, s^{(v)}) \right) \\
 & + \left( (\mathcal{R}(u, v) - \mathcal{R}(u_h, v_h), 2as^{(u)} + bs^{(v)}) + (\mathcal{S}(u, v) - \mathcal{S}(u_h, v_h), bs^{(u)} + 2cs^{(v)}) \right). \tag{5.23}
 \end{aligned}$$

It is easy to see that the second term in RHS of above equality can be simplified by (5.21).

Next we handle the second term in LHS of (5.23). Multiply (5.14) and (5.15) with test functions  $y^{(u)}$  and  $-w^{(u)}$  respectively and integrate

$$\sum_{j=1}^N \left( w^{(u)}, y^{(u)} \right)_{I_j} - \mathcal{D}^+(y^{(u)}, y^{(u)}) = \sum_{j=1}^N \left( \theta^{(u)}, y^{(u)} \right)_{I_j} - \mathcal{D}^+(\gamma^{(u)}, y^{(u)}), \tag{5.24}$$

$$- \sum_{j=1}^N \left( y^{(u)}, w^{(u)} \right)_{I_j} + \mathcal{D}^-(s^{(u)}, w^{(u)}) = - \sum_{j=1}^N \left( \gamma^{(u)}, w^{(u)} \right)_{I_j} + \mathcal{D}^-(\eta^{(u)}, w^{(u)}). \tag{5.25}$$

After applying the equalities in (2.35), (5.19), (5.20) and (5.21), adding (5.24) and (5.25) together, then we have

$$\mathcal{D}^-(s^{(u)}, w^{(u)}) = - \sum_{j=1}^N \left( \frac{1}{2} [y^{(u)}]^2 \right)_{j-\frac{1}{2}} + \sum_{j=1}^N \left( (\gamma^{(u)})^+ [y^{(u)}] \right)_{j-\frac{1}{2}}. \tag{5.26}$$

The analogous result for the Eq. (5.17) and (5.18) with test functions  $y^{(v)}$  and  $-w^{(v)}$  is as follow

$$\mathcal{D}^-(s^{(v)}, w^{(v)}) = - \sum_{j=1}^N \left( \frac{1}{2} [y^{(v)}]^2 \right)_{j-\frac{1}{2}} + \sum_{j=1}^N \left( (\gamma^{(v)})^+ [y^{(v)}] \right)_{j-\frac{1}{2}}. \tag{5.27}$$

Taking the test functions in four Eqs. (5.14), (5.15), (5.17) and (5.18) as  $y^{(v)}$ ,  $-w^{(v)}$ ,  $y^{(u)}$  and  $-w^{(u)}$ , respectively, and performing similar operations yields

$$\begin{aligned}
 & \mathcal{D}^-(s^{(u)}, w^{(v)}) + \mathcal{D}^-(s^{(v)}, w^{(u)}) \\
 & = - \sum_{j=1}^N \left( [y^{(u)}][y^{(v)}] \right)_{j-\frac{1}{2}} + \sum_{j=1}^N \left( (\gamma^{(u)})^+ [y^{(v)}] \right)_{j-\frac{1}{2}} + \sum_{j=1}^N \left( (\gamma^{(v)})^+ [y^{(u)}] \right)_{j-\frac{1}{2}}. \tag{5.28}
 \end{aligned}$$

By virtue of the results in (5.26), (5.27) and (5.28), we add

$$2a\mathcal{D}^-(s^{(u)}, w^{(u)}) + b(\mathcal{D}^-(s^{(u)}, w^{(v)}) + \mathcal{D}^-(s^{(v)}, w^{(u)})) + 2c\mathcal{D}^-(s^{(v)}, w^{(v)})$$

to the second term in the LHS of (5.23) and then get the following important energy equality

$$\begin{aligned}
 & \frac{d}{dt} \mathcal{H}(s^{(u)}, s^{(v)}) + \sum_{j=1}^N \left( a \left( [y^{(u)}]^2 \right)_{j-\frac{1}{2}} + b \left( [y^{(u)}][y^{(v)}] \right)_{j-\frac{1}{2}} + c \left( [y^{(v)}]^2 \right)_{j-\frac{1}{2}} \right) \\
 & - \sum_{j=1}^N \left( 2a \left( (\gamma^{(u)})^+ [y^{(u)}] \right)_{j-\frac{1}{2}} + b \left( (\gamma^{(u)})^+ [y^{(v)}] + (\gamma^{(v)})^+ [y^{(u)}] \right)_{j-\frac{1}{2}} \right. \\
 & \left. + 2c \left( (\gamma^{(v)})^+ [y^{(v)}] \right)_{j-\frac{1}{2}} \right) \\
 & = \sum_{j=1}^N \left( 2a \left( \eta_t^{(u)}, s^{(u)} \right)_{I_j} + b \left( \eta_t^{(u)}, s^{(v)} \right)_{I_j} + b \left( \eta_t^{(v)}, s^{(u)} \right)_{I_j} + 2c \left( \eta_t^{(v)}, s^{(v)} \right)_{I_j} \right)
 \end{aligned}$$

$$\begin{aligned}
 & - \sum_{j=1}^N \left( 2a \left( (\theta^{(u)})^+ [s^{(u)}] \right)_{j-\frac{1}{2}} + b \left( (\theta^{(u)})^+ [s^{(v)}] + (\theta^{(v)})^+ [s^{(u)}] \right)_{j-\frac{1}{2}} \right. \\
 & \quad \left. + 2c \left( (\theta^{(v)})^+ [s^{(v)}] \right)_{j-\frac{1}{2}} \right) \\
 & \quad + \left( \mathcal{R}(u, v) - \mathcal{R}(u_h, v_h), 2as^{(u)} + bs^{(v)} \right) + \left( \mathcal{S}(u, v) - \mathcal{S}(u_h, v_h), bs^{(u)} \right. \\
 & \quad \left. + 2cs^{(v)} \right), \tag{5.29}
 \end{aligned}$$

and we write the above equality as follow for convenience

$$\mathcal{H}_t + \mathcal{O}_0 + \mathcal{O}_1 = \mathcal{O}_2 + \mathcal{O}_3 + \mathcal{O}_n, \tag{5.30}$$

where

$$\mathcal{O}_0 = \sum_{j=1}^N \left( a \left( [y^{(u)}]^2 \right)_{j-\frac{1}{2}} + b \left( [y^{(u)}][y^{(v)}] \right)_{j-\frac{1}{2}} + c \left( [y^{(v)}]^2 \right)_{j-\frac{1}{2}} \right), \tag{5.31}$$

$$\begin{aligned}
 \mathcal{O}_1 = & - \sum_{j=1}^N \left( 2a \left( (\gamma^{(u)})^+ [y^{(u)}] \right)_{j-\frac{1}{2}} + b \left( (\gamma^{(u)})^+ [y^{(v)}] + (\gamma^{(v)})^+ [y^{(u)}] \right)_{j-\frac{1}{2}} \right. \\
 & \left. + 2c \left( (\gamma^{(v)})^+ [y^{(v)}] \right)_{j-\frac{1}{2}} \right), \tag{5.32}
 \end{aligned}$$

$$\mathcal{O}_2 = \sum_{j=1}^N \left( 2a \left( \eta_t^{(u)}, s^{(u)} \right)_{I_j} + b \left( \eta_t^{(u)}, s^{(v)} \right)_{I_j} + b \left( \eta_t^{(v)}, s^{(u)} \right)_{I_j} + 2c \left( \eta_t^{(v)}, s^{(v)} \right)_{I_j} \right), \tag{5.33}$$

$$\begin{aligned}
 \mathcal{O}_3 = & - \sum_{j=1}^N \left( 2a \left( (\theta^{(u)})^+ [s^{(u)}] \right)_{j-\frac{1}{2}} + b \left( (\theta^{(u)})^+ [s^{(v)}] + (\theta^{(v)})^+ [s^{(u)}] \right)_{j-\frac{1}{2}} \right. \\
 & \left. + 2c \left( (\theta^{(v)})^+ [s^{(v)}] \right)_{j-\frac{1}{2}} \right), \tag{5.34}
 \end{aligned}$$

$$\mathcal{O}_n = \left( \mathcal{R}(u, v) - \mathcal{R}(u_h, v_h), 2as^{(u)} + bs^{(v)} \right) + \left( \mathcal{S}(u, v) - \mathcal{S}(u_h, v_h), bs^{(u)} + 2cs^{(v)} \right). \tag{5.35}$$

### 5.4 Proof of the Main Results

We now turn to give the proof of the conclusions presented in previous subsection by virtue of analyzing every term appeared in the energy equality (5.29).

- Proof of error estimates for the linear parts  $\mathcal{O}_0, \mathcal{O}_1, \mathcal{O}_2$  and  $\mathcal{O}_3$ .** In the energy equality, both  $\mathbf{D}_I\text{-C}_n$  and  $\mathbf{D}_I\text{-D}_n$  schemes share the same linear terms  $\mathcal{O}_0, \mathcal{O}_1, \mathcal{O}_2$  and  $\mathcal{O}_3$ , thus we in advance give the error estimates for these terms.

Firstly, we consider the terms  $\mathcal{O}_0$  and  $\mathcal{O}_1$ . Referring to statement in Remark 4.3, condition (1.5) allows a positive real number  $\alpha$  such that

$$\mathcal{O}_0 \geq \alpha \sum_{j=1}^N \left( \left( [y^{(u)}]^2 \right)_{j-\frac{1}{2}} + \left( [y^{(v)}]^2 \right)_{j-\frac{1}{2}} \right). \tag{5.36}$$

Applying the Young’s inequality  $\xi\zeta \leq \epsilon\xi^2 + \frac{1}{4\epsilon}\zeta^2$  with the positive parameter

$$\epsilon = \frac{\alpha}{2 \max(|2a + b|, |b + 2c|)}$$

and interpolation properties to  $\mathcal{O}_1$ , we have

$$\mathcal{O}_1 \geq -\frac{\alpha}{2} \sum_{j=1}^N \left( ([y^{(u)}]^2)_{j-\frac{1}{2}} + ([y^{(v)}]^2)_{j-\frac{1}{2}} \right) - Ch^{2k+1}. \tag{5.37}$$

As a consequence,

$$\mathcal{O}_0 + \mathcal{O}_1 \geq \frac{\alpha}{2} \sum_{j=1}^N \left( ([y^{(u)}]^2)_{j-\frac{1}{2}} + ([y^{(v)}]^2)_{j-\frac{1}{2}} \right) - Ch^{2k+1}. \tag{5.38}$$

Thus we get the following inequality

$$\begin{aligned} \mathcal{H}_t - Ch^{2k+1} &\leq \mathcal{H}_t + \frac{\alpha}{2} \sum_{j=1}^N \left( ([y^{(u)}]^2)_{j-\frac{1}{2}} + ([y^{(v)}]^2)_{j-\frac{1}{2}} \right) - Ch^{2k+1} \\ &\leq \mathcal{H}_t + \mathcal{O}_0 + \mathcal{O}_1. \end{aligned} \tag{5.39}$$

Now we turn to the RHS of the energy equality (5.29). Since the time derivative commutes with the projection  $\mathcal{P}^-$ , we have the following estimate for  $\mathcal{O}_2$

$$|\mathcal{O}_2| \leq Ch^{2k+2} + C(\|s^{(u)}\|^2 + \|s^{(v)}\|^2). \tag{5.40}$$

Moreover,  $\mathcal{O}_3$  can be estimated by the inverse inequalities (5.9) and interpolation properties (5.8) as

$$|\mathcal{O}_3| \leq C(\|s^{(u)}\|^2 + \|s^{(v)}\|^2) + Ch^{2k}, \tag{5.41}$$

or additively by the Young’s inequality

$$|\mathcal{O}_3| \leq \epsilon \sum_{j=1}^N \left( [s^{(u)}]^2 + [s^{(v)}]^2 \right)_{j-\frac{1}{2}} + Ch^{2k+1}, \tag{5.42}$$

here the positive parameter  $\epsilon$  can be chosen small enough according to our need. We remark that these two different versions listed here will be used in two different schemes.

- **Proof of error estimates for  $\mathbf{D}_l\text{-C}_n$  scheme.** In this part, inspired by the work in [5], we analyze the nonlinear term  $\mathcal{O}_n$  with conservative numerical fluxes (3.11) and then complete the error estimates for the  $\mathbf{D}_l\text{-C}_n$  scheme.

Denote

$$\pi^{(u)} = \mathcal{P}^-u, \quad \pi^{(v)} = \mathcal{P}^-v \tag{5.43}$$

for concision and rewrite  $\mathcal{O}_n$  into

$$\begin{aligned} \mathcal{O}_n &= - \left( (\mathcal{R}_c(u_h, v_h) - \mathcal{R}_c(\pi^{(u)}, \pi^{(v)}), 2as^{(u)} + bs^{(v)}) \right. \\ &\quad \left. + (\mathcal{S}_c(u_h, v_h) - \mathcal{S}_c(\pi^{(u)}, \pi^{(v)}), bs^{(u)} + 2cs^{(v)}) \right) \\ &\quad + \left( (\mathcal{R}_c(u, v) - \mathcal{R}_c(\pi^{(u)}, \pi^{(v)}), 2as^{(u)} + bs^{(v)}) \right) \end{aligned}$$

$$\begin{aligned}
 &+ (\mathcal{I}_c(u, v) - \mathcal{I}_c(\pi^{(u)}, \pi^{(v)}), bs^{(u)} + 2cs^{(v)}) \\
 &:= \mathcal{O}_4 + \mathcal{O}_5,
 \end{aligned}
 \tag{5.44}$$

here we have chosen  $\mathcal{R} = \mathcal{R}_c$  and  $\mathcal{S} = \mathcal{I}_c$  in  $\mathcal{O}_n$  in the  $\mathbf{D}_l\text{-C}_n$  scheme.

Recall the form  $\mathcal{R}_c$  and  $\mathcal{I}_c$ , namely,

$$\begin{aligned}
 \mathcal{R}_c(u_h, v_h) - \mathcal{R}_c(\pi^{(u)}, \pi^{(v)}) &= A(\mathcal{N}_c(u_h, u_h) - \mathcal{N}_c(\pi^{(u)}, \pi^{(u)})) \\
 &\quad + B(\mathcal{N}_c(u_h, v_h) - \mathcal{N}_c(\pi^{(u)}, \pi^{(v)})) \\
 &\quad + C(\mathcal{N}_c(v_h, v_h) - \mathcal{N}_c(\pi^{(v)}, \pi^{(v)}))
 \end{aligned}
 \tag{5.45}$$

$$\begin{aligned}
 \mathcal{I}_c(u_h, v_h) - \mathcal{I}_c(\pi^{(u)}, \pi^{(v)}) &= D(\mathcal{N}_c(u_h, u_h) - \mathcal{N}_c(\pi^{(u)}, \pi^{(u)})) \\
 &\quad + E(\mathcal{N}_c(u_h, v_h) - \mathcal{N}_c(\pi^{(u)}, \pi^{(v)})) \\
 &\quad + F(\mathcal{N}_c(v_h, v_h) - \mathcal{N}_c(\pi^{(v)}, \pi^{(v)})).
 \end{aligned}
 \tag{5.46}$$

Apply  $u_h = s^{(u)} + \pi^{(u)}$  and  $v_h = s^{(v)} + \pi^{(v)}$  in the bilinear operator  $\mathcal{N}_c$ , then we have following relations

$$\begin{aligned}
 \mathcal{N}_c(u_h, u_h) - \mathcal{N}_c(\pi^{(u)}, \pi^{(u)}) &= \mathcal{N}_c(s^{(u)}, s^{(u)}) + 2\mathcal{N}_c(s^{(u)}, \pi^{(u)}), \\
 \mathcal{N}_c(v_h, v_h) - \mathcal{N}_c(\pi^{(v)}, \pi^{(v)}) &= \mathcal{N}_c(s^{(v)}, s^{(v)}) + 2\mathcal{N}_c(s^{(v)}, \pi^{(v)}), \\
 \mathcal{N}_c(u_h, v_h) - \mathcal{N}_c(\pi^{(u)}, \pi^{(v)}) &= \mathcal{N}_c(s^{(u)}, s^{(v)}) + \mathcal{N}_c(s^{(u)}, \pi^{(v)}) + \mathcal{N}_c(s^{(v)}, \pi^{(u)}).
 \end{aligned}
 \tag{5.47}$$

Substituting the above transformations into (5.45) and (5.46), we obtain

$$\begin{aligned}
 \mathcal{O}_4 &= -\mathcal{I}_c(s^{(u)}, s^{(v)}) \\
 &\quad - \left( (4Aa + 2Db)\mathcal{N}_c(\pi^{(u)}, s^{(u)}; s^{(u)}) + (2Bb + Eb)\mathcal{N}_c(\pi^{(v)}, s^{(u)}; s^{(u)}) \right. \\
 &\quad \left. + (Bb + 2Ec)\mathcal{N}_c(\pi^{(u)}, s^{(v)}; s^{(v)}) + (2Cb + 4Fc)\mathcal{N}_c(\pi^{(v)}, s^{(v)}; s^{(v)}) \right) \\
 &\quad - \left( (2Ba + Eb)\mathcal{N}_c(\pi^{(u)}, s^{(v)}; s^{(u)}) + (2Ab + 4Dc)\mathcal{N}_c(\pi^{(u)}, s^{(u)}; s^{(v)}) \right. \\
 &\quad \left. + (4Ca + 2Fb)\mathcal{N}_c(\pi^{(v)}, s^{(v)}; s^{(u)}) + (Bb + 2Ec)\mathcal{N}_c(\pi^{(v)}, s^{(u)}; s^{(v)}) \right) \\
 &:= -\mathcal{I}_c(s^{(u)}, s^{(v)}) + \mathcal{O}_{4,1} + \mathcal{O}_{4,2}.
 \end{aligned}
 \tag{5.48}$$

According to Lemma 4.4, we know  $\mathcal{I}_c(s^{(u)}, s^{(v)}) = 0$ . Then applying the property of  $\mathcal{N}_c$  in (2.15), the general form  $\mathcal{N}_c(\pi^{(\zeta)}, s^{(\chi)}; s^{(\chi)})$  of the nonlinear terms in  $\mathcal{O}_{4,1}$ , where  $\zeta$  and  $\chi$  can be  $u$  or  $v$ , is bounded by

$$\begin{aligned}
 |\mathcal{N}_c(\pi^{(\zeta)}, s^{(\chi)}; s^{(\chi)})| &= \frac{1}{2} |\mathcal{N}_c(s^{(\chi)}, s^{(\chi)}; \pi^{(\zeta)})| \\
 &\leq \frac{1}{2} \left( \left| \sum_{j=1}^N \left( (s^{(\chi)})^2, \pi_x^{(\zeta)} \right)_{I_j} \right| + \left| \sum_{j=1}^N \left( \hat{f}(s^{(\chi)}, s^{(\chi)})[\pi^{(\zeta)}] \right)_{j-\frac{1}{2}} \right| \right) \\
 &\leq C(\|\pi_x^{(\zeta)}\|_\infty + h^{-1}\|\eta^{(\zeta)}\|_\infty)\|s^{(\chi)}\|^2,
 \end{aligned}
 \tag{5.49}$$

here the last inequality is deduced from the fact  $[\pi^{(\zeta)}] = [\zeta - \pi^{(\zeta)}] = [\eta^{(\zeta)}]$ . Applying the interpolation property of the projection  $\mathcal{P}^-$  and the smoothness of  $u$  and  $v$ , we can get a constant boundary for  $\|\pi_x^{(\zeta)}\|_\infty + h^{-1}\|\eta^{(\zeta)}\|_\infty$ . Thus we get the estimate for  $\mathcal{O}_{4,1}$

$$|\mathcal{O}_{4,1}| \leq C(\|s^{(u)}\|^2 + \|s^{(v)}\|^2).
 \tag{5.50}$$

Next we turn to  $\mathcal{O}_{4,2}$ . Regarding to condition (1.4), i.e.,

$$\begin{aligned} 2Ea + Eb &= 2Ab + 4Dc, \\ 4Ca + 2Fb &= Bb + 2Ec, \end{aligned}$$

symmetry of  $\mathcal{N}_c(\cdot, \cdot; \zeta)$  and (2.14),  $\mathcal{O}_{4,2}$  can be simplified as follow

$$\begin{aligned} \mathcal{O}_{4,2} &= -(2Ba + Eb)(\mathcal{N}_c(\pi^{(u)}, s^{(v)}; s^{(u)}) + \mathcal{N}_c(\pi^{(u)}, s^{(u)}; s^{(v)})) \\ &\quad - (4Ca + 2Fb)(\mathcal{N}_c(\pi^{(v)}, s^{(v)}; s^{(u)}) + \mathcal{N}_c(\pi^{(v)}, s^{(u)}; s^{(v)})) \\ &= -(2Ba + Eb)(\mathcal{N}_c(\pi^{(u)}, s^{(v)}; s^{(u)}) + \mathcal{N}_c(s^{(u)}, \pi^{(u)}; s^{(v)})) \\ &\quad - (4Ca + 2Fb)(\mathcal{N}_c(\pi^{(v)}, s^{(v)}; s^{(u)}) + \mathcal{N}_c(s^{(u)}, \pi^{(v)}; s^{(v)})) \\ &= (2Ba + Eb)\mathcal{N}_c(s^{(v)}, s^{(u)}; \pi^{(u)}) + (4Ca + 2Fb)\mathcal{N}_c(s^{(v)}, s^{(u)}; \pi^{(v)}). \end{aligned}$$

We can reuse the similar technical skills in (5.49) and then obtain the estimate for  $\mathcal{O}_{4,2}$

$$|\mathcal{O}_{4,2}| \leq C(\|s^{(u)}\|^2 + \|s^{(v)}\|^2). \tag{5.51}$$

Combining (5.50) and (5.51), we then get

$$|\mathcal{O}_4| \leq C(\|s^{(u)}\|^2 + \|s^{(v)}\|^2). \tag{5.52}$$

It remains to show the estimate for the last term  $\mathcal{O}_5$ . Apply  $\pi^{(u)} = u - \eta^{(u)}$  and  $\pi^{(v)} = v - \eta^{(v)}$  to  $\mathcal{N}_c$  in  $\mathcal{O}_5$ , we get

$$\begin{aligned} \mathcal{N}_c(u, u) - \mathcal{N}_c(\pi^{(u)}, \pi^{(u)}) &= 2\mathcal{N}_c(\eta^{(u)}, \pi^{(u)}) - \mathcal{N}_c(\eta^{(u)}, \eta^{(u)}), \\ \mathcal{N}_c(v, v) - \mathcal{N}_c(\pi^{(v)}, \pi^{(v)}) &= 2\mathcal{N}_c(\eta^{(v)}, \pi^{(v)}) - \mathcal{N}_c(\eta^{(v)}, \eta^{(v)}), \\ \mathcal{N}_c(u, v) - \mathcal{N}_c(\pi^{(u)}, \pi^{(v)}) &= \mathcal{N}_c(\eta^{(u)}, \pi^{(v)}) + \mathcal{N}_c(\eta^{(v)}, \pi^{(u)}) - \mathcal{N}_c(\eta^{(u)}, \eta^{(v)}). \end{aligned} \tag{5.53}$$

Substituting the above relations into  $\mathcal{O}_5$ , then  $\mathcal{O}_5$  becomes a sum of two types of nonlinear forms,  $\mathcal{N}_c(\eta^{(\chi)}, \eta^{(\zeta)}; s^{(\kappa)})$  and  $\mathcal{N}_c(\chi, \eta^{(\zeta)}; s^{(\kappa)})$ , here the constants are ignored before them and  $\chi, \zeta, \kappa$  can be  $u$  or  $v$ . For these two forms, we use the inverse inequalities (5.9) and the interpolation properties (5.8) aforementioned and get

$$\begin{aligned} |\mathcal{N}_c(\eta^{(\chi)}, \eta^{(\zeta)}; s^{(\kappa)})| &\leq \sum_{j=1}^N |(\eta^{(\chi)}\eta^{(\zeta)}, s_x^{(\kappa)})_{I_j}| + \sum_{j=1}^N |(\hat{f}(\eta^{(\chi)}, \eta^{(\zeta)})[s^{(\kappa)}])_{j-\frac{1}{2}}| \\ &\leq C\|\eta^{(\chi)}\|_\infty\|\eta^{(\zeta)}\|\|s_x^{(\kappa)}\| + C\|\eta^{(\chi)}\|_\infty\|\eta^{(\zeta)}\|_{L^2(\mathcal{T}_h)}\|s^{(\kappa)}\|_{L^2(\mathcal{T}_h)} \\ &\leq Ch^{2k+1}\|s^{(\kappa)}\|. \end{aligned} \tag{5.54}$$

The fact that  $\|\chi\|_\infty$  is bounded for smooth solution  $\chi$  leads to

$$\begin{aligned} |\mathcal{N}_c(\chi, \eta^{(\zeta)}; s^{(\kappa)})| &\leq \sum_{j=1}^N |(\chi\eta^{(\zeta)}, s_x^{(\kappa)})_{I_j}| + \sum_{j=1}^N |(\hat{f}(\chi, \eta^{(\zeta)})[s^{(\kappa)}])_{j-\frac{1}{2}}| \\ &\leq C\|\eta^{(\zeta)}\|\|s_x^{(\kappa)}\| + C\|\eta^{(\zeta)}\|_{L^2(\mathcal{T}_h)}\|s^{(\kappa)}\|_{L^2(\mathcal{T}_h)} \\ &\leq Ch^k\|s^{(\kappa)}\|. \end{aligned} \tag{5.55}$$

Applying (5.54) and (5.55) in  $\mathcal{O}_5$ , we get the estimate for it

$$|\mathcal{O}_5| \leq Ch^k(\|s^{(u)}\| + \|s^{(v)}\|). \tag{5.56}$$

Finally, combining the estimates for all terms (5.39), (5.40), (5.41), (5.52) and (5.56) together

$$\frac{d}{dt} \mathcal{H}(s^{(u)}, s^{(v)}) \leq C(\|s^{(u)}\|^2 + \|s^{(v)}\|^2) + Ch^{2k}. \tag{5.57}$$

Recalling condition (1.5), there exists a positive number  $\alpha$  such that  $\alpha(\|s^{(u)}\|^2 + \|s^{(v)}\|^2) \leq \mathcal{H}(s^{(u)}, s^{(v)})$ ,

$$\mathcal{H}_t \leq C\mathcal{H} + Ch^{2k}. \tag{5.58}$$

Then the Gronwall’s inequality implies

$$\mathcal{H}(s^{(u)}, s^{(v)}) \leq Ch^{2k}. \tag{5.59}$$

Finally, the desired error estimate (5.10) follows the similar discussion in (4.6).

**Proof of error estimates for  $\mathbf{D}_l\text{-}\mathbf{D}_n$  scheme.** In this part, we turn to complete the error estimates for the  $\mathbf{D}_l\text{-}\mathbf{D}_n$  scheme for the KdV-type system.

Denote  $\mathcal{K} = (S, R)^T$ , then we rewrite the dissipative numerical fluxes defined in (3.12) into following vector form

$$\begin{aligned} \widehat{\mathcal{K}}(\mathbf{p}^-, \mathbf{p}^+) &= \{\mathcal{K}\} - \frac{\varepsilon}{2}[\mathbf{p}] = \frac{\mathcal{K}(\mathbf{p}^+) - \varepsilon\mathbf{p}^+}{2} + \frac{\mathcal{K}(\mathbf{p}^-) + \varepsilon\mathbf{p}^-}{2} \\ &:= \mathcal{K}_+(\mathbf{p}^+) + \mathcal{K}_-(\mathbf{p}^-), \end{aligned} \tag{5.60}$$

with the parameter  $\varepsilon$  satisfying

$$\varepsilon \geq \varrho_0(\mathbb{J}\mathcal{K}), \tag{5.61}$$

where  $\varrho_0(\mathbb{J}\mathcal{K})$  is the maximum spectral radius of the Jacobian matrix  $\frac{\partial(R,S)}{\partial(u,v)}$ . The split two parts  $\mathcal{K}_+(\mathbf{p})$  and  $\mathcal{K}_-(\mathbf{p})$  satisfy that

$$\frac{\partial\mathcal{K}_+(\mathbf{p})}{\partial\mathbf{p}} \leq 0, \quad \frac{\partial\mathcal{K}_-(\mathbf{p})}{\partial\mathbf{p}} \geq 0. \tag{5.62}$$

Here  $\geq 0$  ( $\leq 0$ ) means each eigenvalue is larger (or less) or equal to 0.

Recall the matrix  $\mathbf{M} = \begin{pmatrix} 2a & b \\ b & 2c \end{pmatrix}$ , then further define the fluxes

$$\mathcal{B} = \begin{pmatrix} P(u, v) \\ Q(u, v) \end{pmatrix} = \begin{pmatrix} 2a & b \\ b & 2c \end{pmatrix} \begin{pmatrix} R(u, v) \\ S(u, v) \end{pmatrix}, \tag{5.63}$$

with the corresponding numerical fluxes

$$\widehat{\mathcal{B}} = \begin{pmatrix} \widehat{P}(u, v) \\ \widehat{Q}(u, v) \end{pmatrix} = \begin{pmatrix} 2a & b \\ b & 2c \end{pmatrix} \begin{pmatrix} \widehat{R}(u, v) \\ \widehat{S}(u, v) \end{pmatrix}. \tag{5.64}$$

Condition (1.5) guarantees that property (5.62) for  $\widehat{\mathcal{B}}$  still holds, i.e.,

$$\frac{\partial\mathcal{B}_+(\mathbf{p})}{\partial\mathbf{p}} \leq 0, \quad \frac{\partial\mathcal{B}_-(\mathbf{p})}{\partial\mathbf{p}} \geq 0, \tag{5.65}$$

since  $\mathcal{B} = \mathbf{M}\mathcal{K}$  and the Jacobian matrix  $\frac{\partial\mathcal{B}_-(\mathbf{p})}{\partial\mathbf{p}}$  (or  $\frac{\partial\mathcal{B}_+(\mathbf{p})}{\partial\mathbf{p}}$ ) keeps its eigenvalues being non-negative (or non-positive) when multiplied by a positive definitive matrix  $\mathbf{M}$ . Furthermore, the transformation in (5.63) leads to some desired symmetric property of  $\mathcal{B}$ , i.e.,

$$\frac{\partial\mathcal{B}}{\partial\mathbf{p}} = \begin{pmatrix} \partial_u P & \partial_v P \\ \partial_u Q & \partial_v Q \end{pmatrix} = \begin{pmatrix} 2a & b \\ b & 2c \end{pmatrix} \begin{pmatrix} 2Au + Bv & Bu + 2Cv \\ 2Du + Ev & Eu + 2Fv \end{pmatrix}$$

$$= \begin{pmatrix} (4aA + 2bD)u + (2aB + bE)v & (2aB + bE)u + (2bF + 4aC)v \\ (2bA + 4cD)u + (bB + 2cE)v & (bB + 2cE)u + (2bC + 4cF)v \end{pmatrix}. \tag{5.66}$$

On account of the fact that  $a, b$  and  $c$  satisfy condition (1.4), we have

$$(2bA + 4cD)u + (bB + 2cE)v = (2aB + bE)u + (2bF + 4aC)v, \tag{5.67}$$

which means that the Jacobian matrix  $\mathbb{J}_{\mathcal{B}}$  is symmetric. Therefore  $\widehat{\mathcal{B}}$  is an E-flux since  $\mathcal{B}$  is symmetric and the property (5.65) holds.

In addition, we would like to use the a priori technique below. To deal with the nonlinearity of  $\mathcal{B}$ , we assume a priori that for  $h$  sufficiently small then there holds

$$\|\mathbf{p} - \mathbf{p}_h\| \leq h. \tag{5.68}$$

This is obviously true for  $t = 0$  by  $\mathbf{p}_h(x, 0) = \mathcal{P}\mathbf{p}_0(x)$ , where  $\mathcal{P}$  is the standard  $L^2$ -projection to  $V_h$  as defined before. We will verify the correctness of this assumption later. Furthermore, the inverse inequalities (5.9) and the approximation properties (5.8), imply that

$$\|\mathbf{e}\|_\infty \leq Ch^{\frac{1}{2}} \quad \text{and} \quad \|\mathcal{Q}\mathbf{p} - \mathbf{p}_h\|_\infty \leq Ch^{\frac{1}{2}}, \tag{5.69}$$

where  $\mathbf{e} = \mathbf{p} - \mathbf{p}_h$  and  $\mathcal{Q} = \mathcal{P}$  or  $\mathcal{Q} = \mathcal{P}^\pm$  is the projection operator.

Referring to the strategies in handling the E-flux in [30], it is time for us to estimate the nonlinear terms  $\mathcal{O}_n$  in the energy equality (5.29) by taking  $\mathcal{R} = \mathcal{R}_d$  and  $\mathcal{S} = \mathcal{S}_d$

$$\begin{aligned} & (\mathcal{R}_d(u, v) - \mathcal{R}_d(u_h, v_h), 2as^{(u)} + bs^{(v)}) + (\mathcal{S}_d(u, v) - \mathcal{S}_d(u_h, v_h), bs^{(u)} + 2cs^{(v)}) \\ &= \sum_{j=1}^N \int_{I_j} \begin{pmatrix} s_x^{(u)} \\ s_x^{(v)} \end{pmatrix}^T \begin{pmatrix} 2a & b \\ b & 2c \end{pmatrix} \begin{pmatrix} R(u, v) - R(u_h, v_h) \\ S(u, v) - S(u_h, v_h) \end{pmatrix} dx \\ &+ \sum_{j=1}^N \begin{pmatrix} [s^{(u)}] \\ [s^{(v)}] \end{pmatrix}^T_{j-\frac{1}{2}} \begin{pmatrix} 2a & b \\ b & 2c \end{pmatrix} \begin{pmatrix} R(u, v) - \widehat{R}(u_h, v_h) \\ S(u, v) - \widehat{S}(u_h, v_h) \end{pmatrix}_{j-\frac{1}{2}} \\ &= \sum_{j=1}^N \int_{I_j} \begin{pmatrix} s_x^{(u)} \\ s_x^{(v)} \end{pmatrix}^T \begin{pmatrix} P(u, v) - P(u_h, v_h) \\ Q(u, v) - Q(u_h, v_h) \end{pmatrix} dx + \sum_{j=1}^N \begin{pmatrix} [s^{(u)}] \\ [s^{(v)}] \end{pmatrix}^T_{j-\frac{1}{2}} \begin{pmatrix} P(u, v) - P_{ref} \\ Q(u, v) - Q_{ref} \end{pmatrix}_{j-\frac{1}{2}} \\ &+ \sum_{j=1}^N \begin{pmatrix} [s^{(u)}] \\ [s^{(v)}] \end{pmatrix}^T_{j-\frac{1}{2}} \begin{pmatrix} P_{ref} - \widehat{P}(u_h, v_h) \\ Q_{ref} - \widehat{Q}(u_h, v_h) \end{pmatrix}_{j-\frac{1}{2}} \\ &= \sum_{j=1}^N \int_{I_j} \mathbf{s}_x^T (\mathcal{B}(\mathbf{p}) - \mathcal{B}(\mathbf{p}_h)) dx + \sum_{j=1}^N \left( [\mathbf{s}]^T (\mathcal{B}(\mathbf{p}) - \mathcal{B}_{ref}) \right)_{j-\frac{1}{2}} \\ &+ \sum_{j=1}^N \left( [\mathbf{s}]^T (\mathcal{B}_{ref} - \widehat{\mathcal{B}}(\mathbf{p}_h)) \right)_{j-\frac{1}{2}} \\ &:= \Pi_1 + \Pi_2 + \Pi_3, \end{aligned} \tag{5.70}$$

where we denote  $\mathbf{s} = (s^{(u)}, s^{(v)})^T$  and  $\mathcal{B}_{ref} = (P_{ref}, Q_{ref})^T := \frac{1}{6}\mathcal{B}(\mathbf{p}^-) + \frac{2}{3}\mathcal{B}(\{\mathbf{p}\}) + \frac{1}{6}\mathcal{B}(\mathbf{p}^+)$  is a reference vector defined on the element interfaces. Referring to the work in [30], denoting  $\mathbf{e} = \mathbf{p} - \mathbf{p}_h = (e^{(u)}, e^{(v)})^T$  and  $\boldsymbol{\eta} = (\eta^{(u)}, \eta^{(v)})^T$ , we give estimates for the three terms in (5.70) as follows

$$\Pi_1 + \Pi_2 \leq C(\|s^{(u)}\|^2 + \|s^{(v)}\|^2) + (C + C_\star\|\mathbf{e}\|_\infty)h^{2k+1}, \tag{5.71}$$

$$\Pi_3 \leq -\frac{1}{2}\mathcal{A}(\mathbf{p}) + C_\star h^{-1} \|\mathbf{e}\|_\infty^2 (\|s^{(u)}\|^2 + \|s^{(v)}\|^2) + Ch^{2k+1}, \tag{5.72}$$

here the notation  $\mathcal{A}(\mathbf{p}) = \sum_{j=1}^N [\mathbf{p}]_{j-\frac{1}{2}}^T \mathcal{A}(\widehat{\mathcal{B}}; \mathbf{p})_{j-\frac{1}{2}} [\mathbf{p}]_{j-\frac{1}{2}} \geq 0$ . Take the parameter  $\epsilon$  in (5.42) small enough such that the term  $\epsilon (\|s^{(u)}\|^2 + \|s^{(v)}\|^2)$  can be eliminated by  $\frac{1}{4}\mathcal{A}(\mathbf{p})$ , combine the above results with the estimates (5.39), (5.40) and (5.42), then we have

$$\frac{d}{dt} \mathcal{H}(s^{(u)}, s^{(v)}) \leq -\frac{1}{4}\mathcal{A}(\mathbf{p}) + (C + C_\star h^{-1} \|\mathbf{e}\|_\infty^2) (\|s^{(u)}\|^2 + \|s^{(v)}\|^2) + (C + C_\star \|\mathbf{e}\|_\infty) h^{2k+1}. \tag{5.73}$$

Applying the property  $\mathcal{A}(\mathbf{p}) \geq 0$  and the a priori assumption (5.69), we finally obtain

$$\frac{d}{dt} \mathcal{H}(s^{(u)}, s^{(v)}) \leq C (\|s^{(u)}\|^2 + \|s^{(v)}\|^2) + Ch^{2k+1}. \tag{5.74}$$

The desired error estimate (5.11) for the  $\mathbf{D}_l$ - $\mathbf{D}_n$  scheme of the KdV-type system eventually comes out by applying the positive definite condition (1.5) along with the same strategy used in last part for the  $\mathbf{D}_l$ - $\mathbf{C}_n$  scheme.

**Remark 5.3** To complete the proof, we turn to justify the verification of the a priori assumption (5.68). For  $k \geq 1$ , we can assume  $h$  sufficiently small such that  $Ch^k < \frac{1}{2}h$  with constant  $C$  determined by the final time  $T$ . Then, denote  $t^* = \sup\{t : \|\mathbf{p}(t) - \mathbf{p}_h(t)\| \leq h\}$ , we would have  $\|\mathbf{p}(t^*) - \mathbf{p}_h(t^*)\| = h$  for continuity if  $t^*$  is finite. On the other hand, the proof tells us that (5.11) holds for  $t \leq t^*$  and then  $\|\mathbf{p}(t^*) - \mathbf{p}_h(t^*)\| \leq Ch^{k+\frac{1}{2}} < \frac{1}{2}h$ . This is a contradiction if  $t^* < T$ . Therefore  $t^* \geq T$  and the a priori assumption (5.68) is verified.

## 6 Numerical Experiments

In what follows, referring to the exhaustive work in [5], we apply the LDG schemes proposed in our paper to several numerical examples of the KdV-type system. Accuracy tests for two kinds of traveling waves, long-time simulations for solitary wave solutions, and interactions of multi-solitary waves are successively presented and compared for different numerical schemes.

The well-known additive Runge–Kutta (ARK) method in [8,20] are used as the temporal discretization in following experiments. In [8], the implicit-explicit additive Runge–Kutta (ARK) methods from third- to fifth-order are presented in which the stiff terms are integrated by an L-stable, stiffly-accurate, singly diagonally implicit Runge–Kutta method while the non-stiff terms are integrated with a traditional explicit Runge–Kutta method. And in [20], we can see the very good qualification of the ARK methods when applied to the LDG methods in simulating (non)linear KdV equations. Therefore, the ARK methods are introduced into our experiments as the temporal discretization of the LDG methods to system (1.1), and it will be numerically verified qualified and efficient in the accuracy tests and long-time interactions simulation of multi-solitary waves. In addition, the time step size will be taken as  $\Delta t = 0.1\Delta x$  in this paper.

We remark that in following experiments, the linear terms with third order derivatives in (1.1) are multiplied by a small parameter  $\epsilon$  to adapt the KdV-type system to the interval  $I = [0, 1]$ , and such change does not affect the conclusions proposed in our paper. The parameters  $A, B, \dots, F$  are chosen as same as in [5]

$$A = \frac{1}{8}, \quad B = \frac{1}{8}, \quad C = \frac{1}{32}, \quad D = \frac{1}{8}, \quad E = 1, \quad F = -\frac{9}{32},$$

and these choices result in the following settings

$$a = \frac{118}{17}, \quad b = -\frac{28}{17}, \quad c = 1,$$

which solve the system (1.4) and satisfy that  $4ac - b^2 = \frac{7240}{289} > 0$ . We remark that the parameter  $b$  is especially chosen negative to verify the capacity of  $C_l-D_n$  or  $D_l-D_n$  scheme, and the discussion about  $a, b, c$  is declared in Remark 4.2 detailedly.

**Example 6.1** Accuracy tests for proportional traveling wave solutions.

The authors in [4] have introduced and analyzed a kind of so-called proportional solitary waves of the form  $(u, v) = (u, 2u)$  for the KdV-type system (1.1). In some sense, this special setting simplifies the system with the coupled nonlinear terms into the classical nonlinear KdV equation. Thus we will always display the numerical results for the variable  $u$  yet omit the other one for  $v = 2u$ . Herein, we introduce two kinds of periodic exact solutions with period 1 to the system and give the accuracy tests for our numerical schemes.

- **The cnoidal-wave solution.** We first take the well known cnoidal-wave solution of the KdV equation

$$u(x, t) = \lambda \text{cn}^2((4K(m)(x - \omega t - x_0) : m), \tag{6.1}$$

where  $\text{cn}(z : m)$  is the Jacobi elliptic function with modulus  $m \in (0, 1)$  and the function  $K = K(m)$  is the complete elliptic integral of the first kind.

The parameters are set as

$$\epsilon = \frac{1}{576}, \quad m = 0.9, \quad \lambda = 192\epsilon m K(m)^2, \quad \omega = 64\epsilon(2m - 1)K(m)^2, \quad x_0 = 0.5. \tag{6.2}$$

- **The solitary-wave solution.** We also introduce the proportional solitary-wave solution with

$$u(x, t) = \Lambda \text{sech}^2(K(x - \omega t - x_0)), \tag{6.3}$$

where

$$\Lambda = 1, \quad \omega = \frac{\Lambda}{3}, \quad \epsilon = \frac{1}{5760}, \quad K = \frac{1}{2}\sqrt{\frac{\Lambda}{3\epsilon}}, \quad x_0 = 0.5. \tag{6.4}$$

Referring to the discussion in [5], the above solitary-wave solution can be regarded as an exact solution of the system owing to the symmetry of the initial profile about its crest ( $x = x_0$ ) and the exponential decay away from its crest.

For these two kinds of traveling wave solutions, we test the accuracy of four semi-discrete LDG schemes presented in this paper equipped with the ARK temporal discretization. The  $L^2$  errors  $\|u - u_h\|$  and relevant orders of accuracy for all schemes simulating the cnoidal-wave solution (6.1) and the solitary-wave solution (6.3) at time  $t = 1$  are showed in Table 2 and Table 3, respectively. The periodic boundary conditions and piecewise polynomials of degree less than or equal to  $k$  on uniform meshes with  $N$  cells are used our methods.

The numerical results show optimal convergence rates for even  $k$  and sub-optimal convergence rates for odd  $k$  in the  $C_l-C_n$  and  $C_l-D_n$  schemes. This kind of phenomenon also appeared in [16,31] when the LDG method is used to solve the generalized KdV equation equipped with the same numerical fluxes as (3.9) for linear terms. Yet convergence rates for

$k$  being odd are optimal in  $\mathbf{D}_l\text{-}\mathbf{C}_n$  and  $\mathbf{D}_l\text{-}\mathbf{D}_n$  schemes when the numerical fluxes (3.11) for linear terms are chosen. Therefore, the principal difference among the four schemes is affected mainly by the choice of numerical fluxes for linear terms  $\mathcal{D}$ .

Besides, the computational efficiency study of the four different schemes is applied to the cnoidal-wave solution by taking the evolution time  $t = 10$ , and the settings of the other parameters are the same as (6.2). The information of the device used in this experiment is as follow

- processor : 2.3 GHz Quad-Core Intel Core i5,
- memory: 8 GB 2133 MHz LPDDR3.

As shown in Table 4, the time-consuming of the four schemes are almost the same. And compared with the degree of polynomials, the scale of the mesh grid plays a dominant role in the computational efficiency of all four LDG schemes.

**Example 6.2** Long-time simulations of the solitary-wave solution.

In this experiment, we study the long-time behaviors of our proposed LDG schemes in simulating the proportional solitary-wave solutions  $(u, v) = (u, 2u)$ . The parameters are set the same as in (6.4). Example 6.1 seems to suggest that the choice of numerical fluxes for linear terms  $\mathcal{D}$  plays an essential role in the performance of all four schemes, therefore we just center on two representative schemes, the  $\mathbf{C}_l\text{-}\mathbf{C}_n$  and  $\mathbf{D}_l\text{-}\mathbf{D}_n$  schemes, in current and future examples.

We use three experiments, in Figs. 1, 2 and 3, to study the performance and comparison about the  $\mathbf{C}_l\text{-}\mathbf{C}_n$  and  $\mathbf{D}_l\text{-}\mathbf{D}_n$  schemes in long-time simulations with varying the values of  $k$  and  $N$ . The profiles of the solitary-wave solutions of  $u$  and  $u_h$  (data for  $v = 2u$  are ignored for concision) at  $t = 250, 500, 750, 1000$  (especially in Fig. 3, at  $t = 500, 1000, 3000, 5000$ ) in addition to the quantities  $|\mathcal{H}(u_h, v_h) - \mathcal{H}(u, v)|$  and the phase errors for the numerical traveling wave solutions are depicted in three figures. And we remark that the phase error of the numerical scheme is a quantity which manifests the lag between locations of the crest of the exact solution  $u$  and its approximation  $u_h$ . For more detailed discussion about the phase error, we refer readers to [5].

The  $P^2$  polynomial element, a uniform mesh with  $N = 80$  cells and the third-order ARK method are used in the first test with results in Fig. 1. In the long-time evolution, we find that the conservative scheme performs better than the dissipative one for it simulating the exact solution more accurate, preserving the invariant  $\mathcal{H}$  with less dissipation and generating smaller phase errors. Furthermore, the dissipative method suffers a loss of amplitude of the solitary wave in a long time. In Fig. 2, we double the number of cells  $N = 160$  and remain other settings to study the improvement led by mesh refinement. It is clear to see that the behaviors of both schemes get some progress especially in the  $\mathbf{D}_l\text{-}\mathbf{D}_n$  scheme overcoming the loss of amplitude and reducing the phase errors tremendously. As a consequence, the invariant  $\mathcal{H}$  is preserved better here than the coarse mesh. In Fig. 3, we alternatively keep the mesh with  $N = 80$  whereas improve the accuracy of schemes by utilizing  $P^4$  polynomial and corresponding fifth-order ARK method and enlarge the end time to  $T = 5000$ . In the first four profiles, the differences between the numerical solutions and the exact solution are invisible to the naked eyes. And the last two subfigures show that  $|\mathcal{H}(u_h, v_h) - \mathcal{H}(u, v)|$  of two schemes are restricted in  $10^{-7} \sim 10^{-5}$  and the phase errors are nearly eliminated. This choice of mesh and polynomials resolves the solitary-wave solution well in the sufficiently long-time simulation. We conclude that the mesh refinement and high accuracy both play important roles in  $\mathbf{C}_l\text{-}\mathbf{C}_n$  and  $\mathbf{D}_l\text{-}\mathbf{D}_n$  schemes applied to long-time simulations of the solitary-wave solution.

**Table 2** Accuracy test for the cnoidal-wave solution (6.1) of the KdV-type system

$k$	$N$	$C_J-C_n$ scheme		$C_J-D_n$ scheme		$D_J-C_n$ scheme		$D_J-D_n$ scheme	
		$L^2$ error	Order						
1	10	6.5810e-01	-	4.0262e-01	-	4.7635e-01	-	5.9557e-01	-
1	20	5.8258e-01	0.18	1.9992e-01	1.01	1.8261e-01	1.38	2.6255e-01	1.18
1	40	3.6782e-01	0.66	6.9550e-02	1.52	4.1188e-02	2.15	5.7142e-02	2.20
1	80	2.0021e-01	0.88	2.0349e-02	1.77	8.6517e-03	2.25	1.0759e-02	2.41
1	160	1.0243e-01	0.97	4.4280e-03	2.20	1.9263e-03	2.17	2.1828e-03	2.30
2	10	7.6303e-02	-	3.2201e-01	-	9.7918e-02	-	1.3009e-01	-
2	20	7.2049e-03	3.40	8.2338e-03	5.29	5.3259e-03	4.20	6.9386e-03	4.23
2	40	3.4275e-04	4.39	3.7105e-04	4.47	4.4881e-04	3.57	4.8125e-04	3.85
2	80	4.1418e-05	3.05	4.2118e-05	3.14	5.1722e-05	3.12	5.2265e-05	3.20
2	160	5.0916e-06	3.02	5.1106e-06	3.04	6.3653e-06	3.02	6.3770e-06	3.03
3	10	3.1702e-02	-	6.2334e-03	-	7.0651e-03	-	9.0747e-03	-
3	20	6.0442e-03	2.39	2.5921e-04	4.59	2.6710e-04	4.73	2.6128e-04	5.12
3	40	8.0696e-04	2.90	2.9197e-05	3.15	1.8400e-05	3.86	1.8293e-05	3.84
3	80	1.0251e-04	2.98	3.4323e-06	3.09	1.1665e-06	3.98	1.1653e-06	3.97
3	160	1.2762e-05	3.01	4.1063e-07	3.06	7.2907e-08	4.00	7.2893e-08	4.00

**Table 3** Accuracy test for the solitary-wave solution (6.3) of the KdV-type system

$k$	$N$	$C_J-C_n$ scheme		$C_J-D_n$ scheme		$D_J-C_n$ scheme		$D_J-D_n$ scheme	
		$L^2$ error	Order						
1	10	1.8766e-01	-	1.2488e-01	-	9.6089e-02	-	1.3650e-01	-
1	20	1.2621e-01	0.57	1.5110e-01	-0.27	1.5414e-01	-0.68	2.0619e-01	-0.60
1	40	8.1249e-02	0.64	8.5727e-02	0.82	6.7969e-02	1.18	1.1494e-01	0.84
1	80	3.5435e-02	1.20	2.8219e-02	1.60	1.5604e-02	2.12	2.7404e-02	2.07
1	160	1.6043e-02	1.14	6.8386e-03	2.04	3.2865e-03	2.25	4.9462e-03	2.47
2	10	2.1062e-01	-	2.2959e-01	-	2.0858e-01	-	2.3950e-01	-
2	20	4.1271e-02	2.35	8.1378e-02	1.50	3.7424e-02	2.48	5.9750e-02	2.00
2	40	3.2961e-03	3.65	7.0533e-03	3.53	1.8856e-03	4.31	3.3965e-03	4.14
2	80	1.0194e-04	5.01	1.3591e-04	5.70	1.3523e-04	3.80	1.7074e-04	4.31
2	160	1.1833e-05	3.11	1.2304e-05	3.47	1.4980e-05	3.17	1.5395e-05	3.47
3	10	7.7663e-02	-	1.3034e-01	-	9.4746e-02	-	1.1839e-01	-
3	20	5.0696e-03	3.94	5.7608e-03	4.50	3.3990e-03	4.80	4.9896e-03	4.57
3	40	1.4635e-03	1.79	8.523e-05	6.07	9.6082e-05	5.14	9.0609e-05	5.78
3	80	1.9573e-04	2.90	9.0194e-06	3.25	6.6925e-06	3.84	6.5664e-06	3.79
3	160	2.4908e-05	2.97	1.0148e-06	3.15	4.3037e-07	3.96	4.2909e-07	3.94

**Table 4** Computational efficiency test

		$C_I-C_n$ scheme		$C_I-D_n$ scheme		$D_I-C_n$ scheme		$D_I-D_n$ scheme	
$k = 2$	$N = 80$	3 min	5 s	2 min	58 s	2 min	57 s	2 min	52 s
$k = 3$	$N = 80$	5 min	6 s	5 min	9 s	4 min	46 s	4 min	40 s
$k = 3$	$N = 160$	18 min	36 s	18 min	18 s	17 min	16 s	16 min	54 s

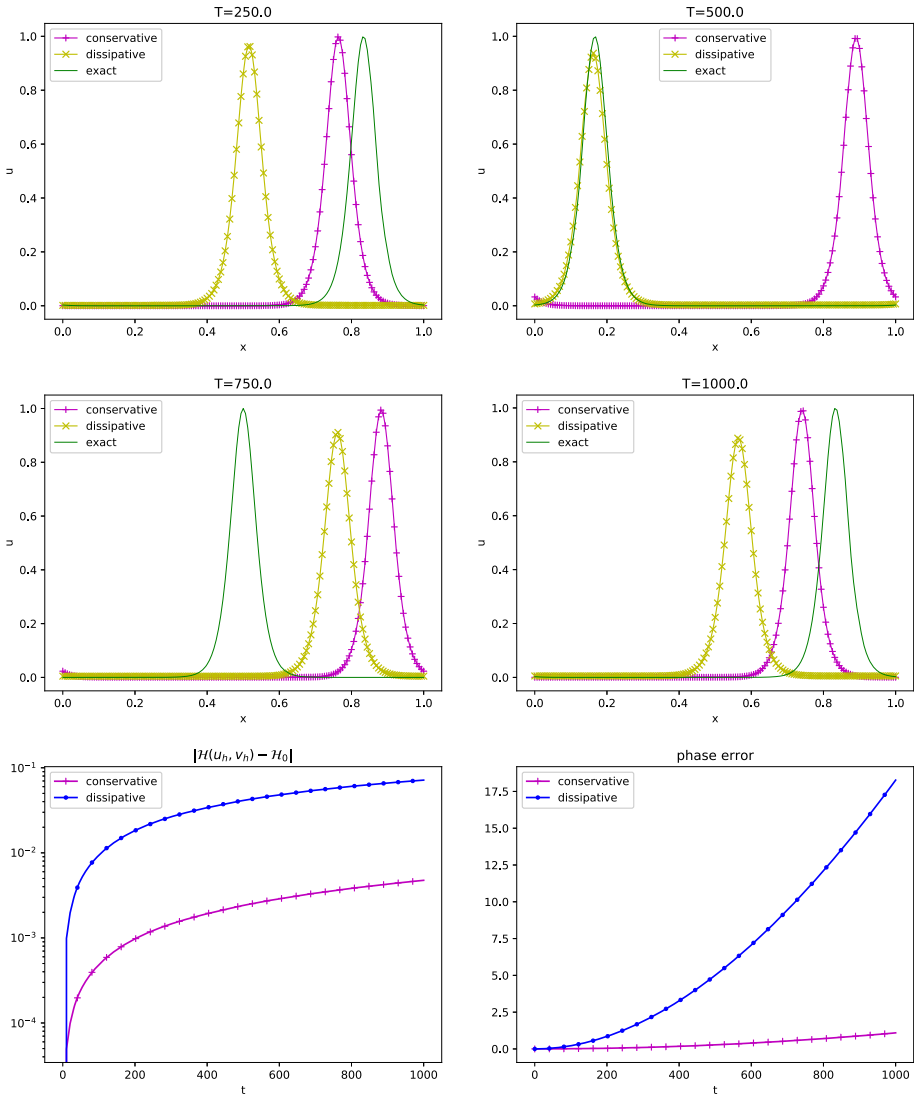


**Fig. 1** The solitary-wave solution (6.3) of  $(x, t) \in [0, 1] \times [0, 1000]$ .  $P^2$  elements and uniform mesh with  $N = 80$  cells. Third-order ARK method

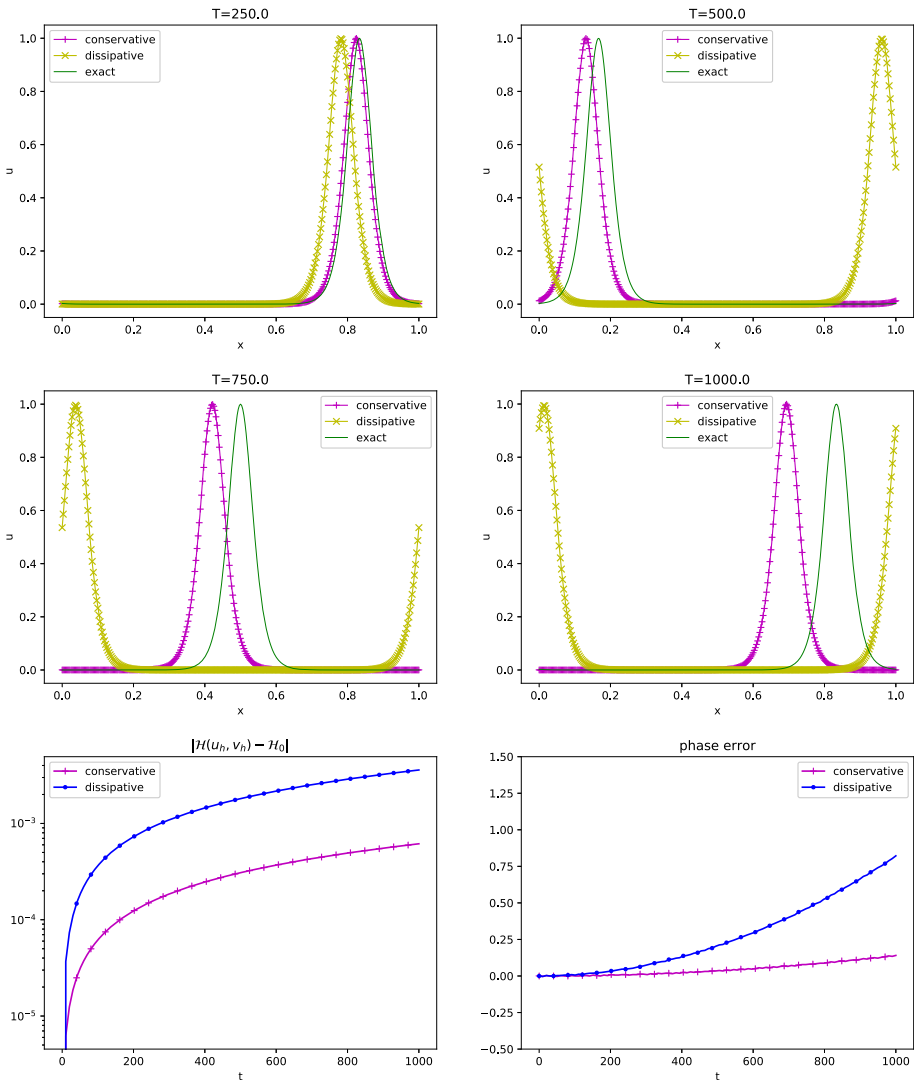


**Fig. 2** The solitary-wave solution (6.3) of  $(x, t) \in [0, 1] \times [0, 1000]$ .  $P^2$  elements and uniform mesh with  $N = 160$  cells. Third-order ARK method

In [17], the authors designed an experiment to investigate the phase error about conservative and dissipative LDG methods to the Benjamin–Bona–Mahony (BBM) equation, and we follow their idea to revisit this issue in the KdV-type system. Comparing to the results in Fig. 1 at  $t = 250, 500, 750$ , which are placed in the left column of Fig. 4, the right column of Fig. 4 provide the numerical results with a half time step size while keeping all the other parameters. After reducing  $\Delta t$ , the phase error about the  $C_l-C_n$  scheme decreases more significantly than the  $D_l-D_n$  scheme. As a consequence, the large phase error of the conservative scheme is mainly caused by the temporal discretization error.

**Example 6.3** Interactions of multi-solitary waves.

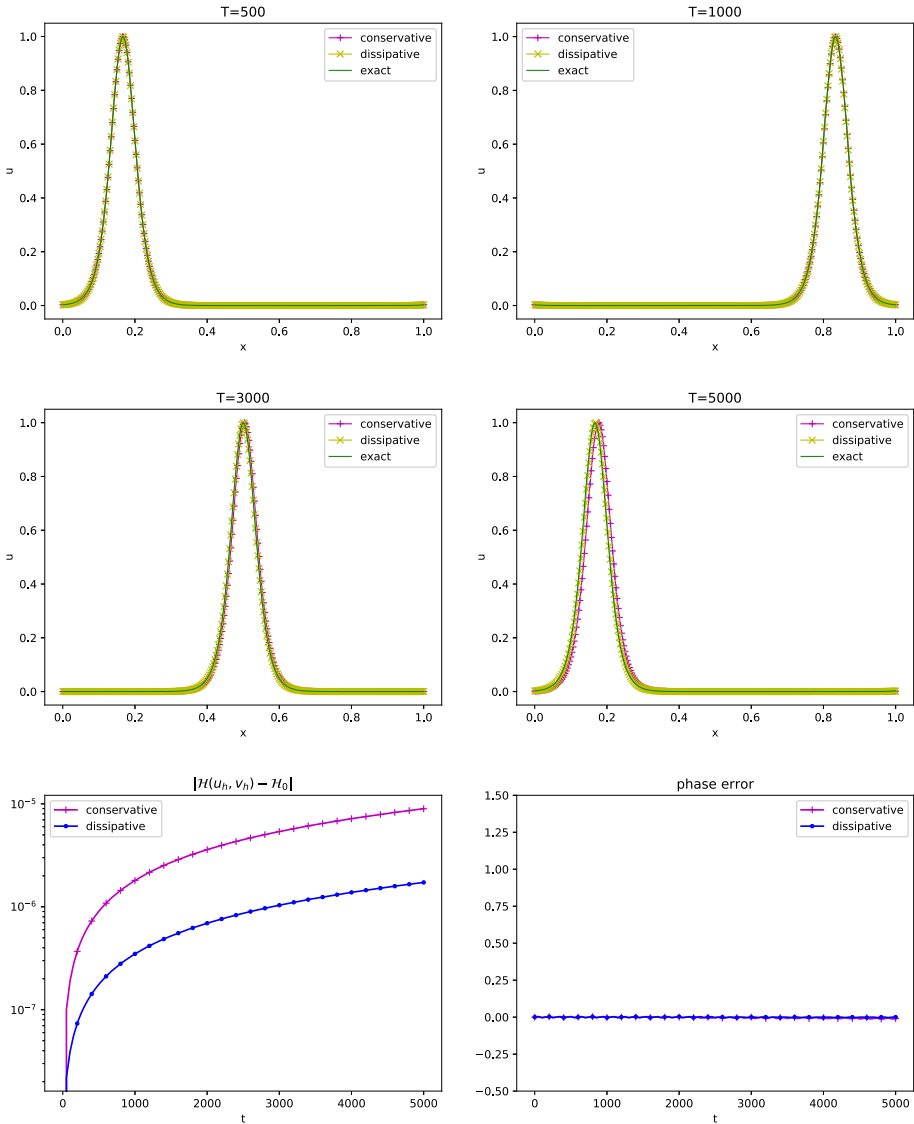


**Fig. 3** The solitary-wave solution (6.3) of  $(x, t) \in [0, 1] \times [0, 5000]$ .  $P^4$  elements and uniform mesh with  $N = 80$  cells. Fifth-order ARK method

In this experiment, we turn to study the interactions of multi-solitary waves, which are the well known phenomena of KdV-type equations. According to the proportional solitary-wave solution (6.3), we enlarge the periodic domain  $[0, 1]$  to  $[0, 10]$  to capture the delicate details and put  $M$  (2 or 3) solitary waves (still the proportional type solution  $(u, v) = (u, 2u)$  for each solitary wave) with different transport speeds and locations

$$u(x, t) = \sum_{i=1}^M \Lambda_i \operatorname{sech}^2(K_i(x - \omega_i t - x_i)). \tag{6.5}$$

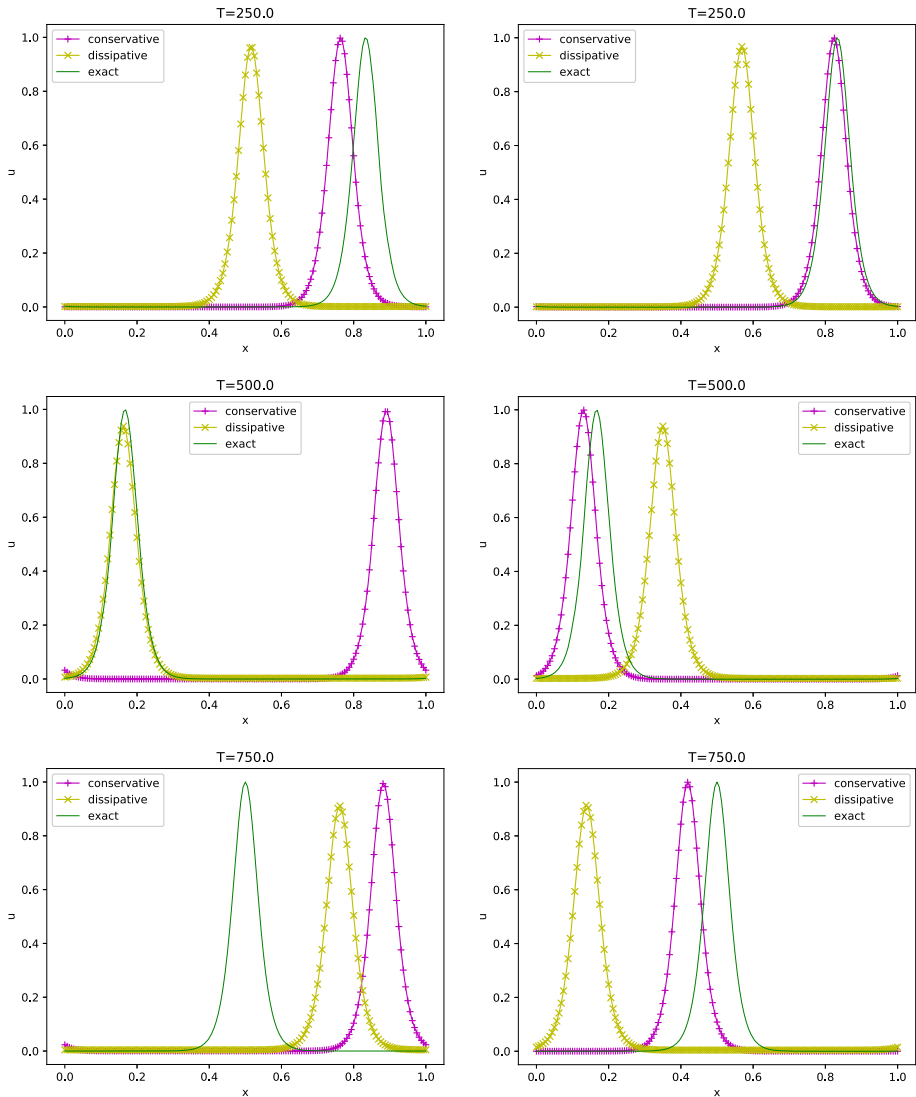


**Fig. 4** The comparison of the solitary-wave of  $C_l-C_n$  and  $D_l-D_n$  schemes at different times  $t = 250$  (top),  $t = 500$  (middle),  $t = 750$  (bottom) with time step  $\Delta t = 1/800$  (left column) and  $\Delta t = 1/1600$  (right column).  $P^2$  elements and uniform mesh with  $N = 80$  cells. Third-order ARK method

Take  $\epsilon = 1/576$  and set the other parameters for two-solitary wave ( $M = 2$ ) as

$$\begin{aligned}
 \Lambda_1 &= 2, & \omega_1 &= \frac{\Lambda_1}{3}, & K_1 &= \frac{1}{2}\sqrt{\frac{\Lambda_1}{3\epsilon}}, & x_1 &= 1, \\
 \Lambda_2 &= 1, & \omega_2 &= \frac{\Lambda_2}{3}, & K_2 &= \frac{1}{2}\sqrt{\frac{\Lambda_2}{3\epsilon}}, & x_2 &= 3,
 \end{aligned}
 \tag{6.6}$$

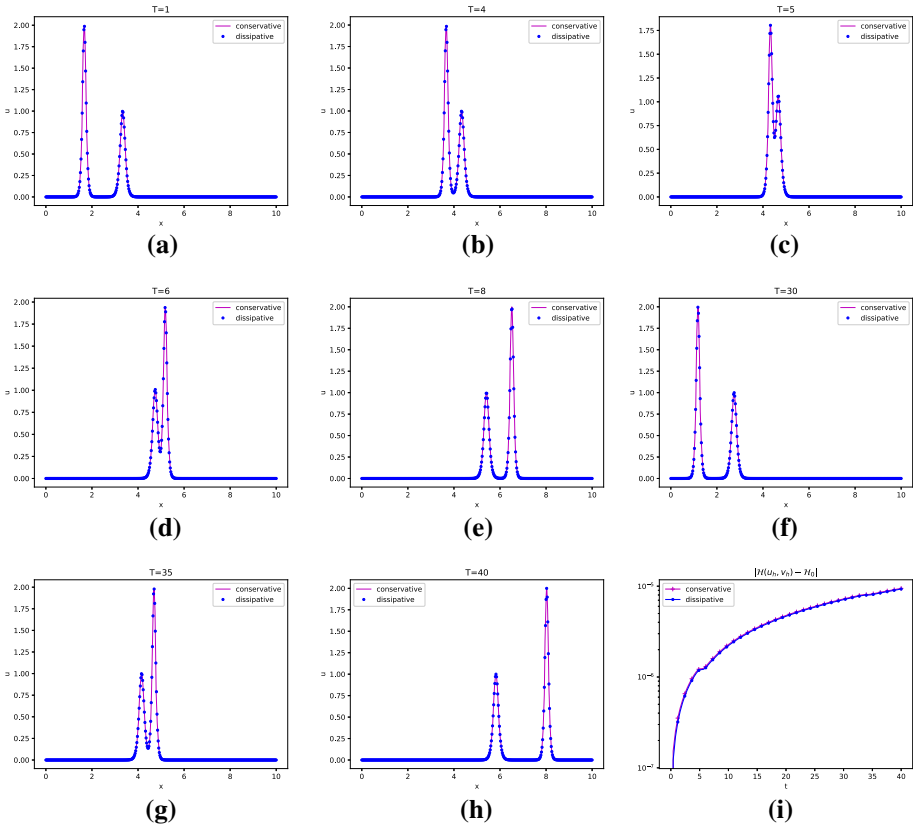


**Fig. 5** The interactions of two-solitary wave (6.5) with parameters (6.6),  $(x, t) \in [0, 10] \times [0, 40]$ .  $P^4$  elements and uniform mesh with  $N = 400$  cells. Fifth-order ARK method. **a–e** depict the first interaction; **f–h** depict the second interaction; **i** shows the  $\mathcal{H}$ -energy evolution in the semilog coordinate

and for three-solitary wave ( $M = 3$ ) as

$$\begin{aligned}
 \Lambda_1 &= 3, & \omega_1 &= \frac{\Lambda_1}{3}, & K_1 &= \frac{1}{2} \sqrt{\frac{\Lambda_1}{3\epsilon}}, & x_1 &= 1, \\
 \Lambda_2 &= 2, & \omega_2 &= \frac{\Lambda_2}{3}, & K_2 &= \frac{1}{2} \sqrt{\frac{\Lambda_2}{3\epsilon}}, & x_2 &= 3, \\
 \Lambda_3 &= 1, & \omega_3 &= \frac{\Lambda_3}{3}, & K_3 &= \frac{1}{2} \sqrt{\frac{\Lambda_3}{3\epsilon}}, & x_3 &= 4.
 \end{aligned}
 \tag{6.7}$$

In the two experiments, the  $P^4$  piecewise polynomials equipped with the corresponding fifth-order ARK temporal discretization methods are applied. Besides, we utilize the meshes with  $N = 400$  (cell size  $h = 1/40$ ) for the two- and three-solitary waves. In Figs. 5 and 6, we show the movements and interactions for these multi-solitary waves in  $t \in [0, 40]$ . The first and second interactions of the two solitons, on account of its periodicity, are depicted in Fig. 5. Analogously in Fig. 6, we show the interactions about three solitons at  $t = 0$  and depict the subsequent behaviors in a relatively long time. It transpires that the solitons simulated by our numerical schemes can efficiently separate from each other after the interactions, and

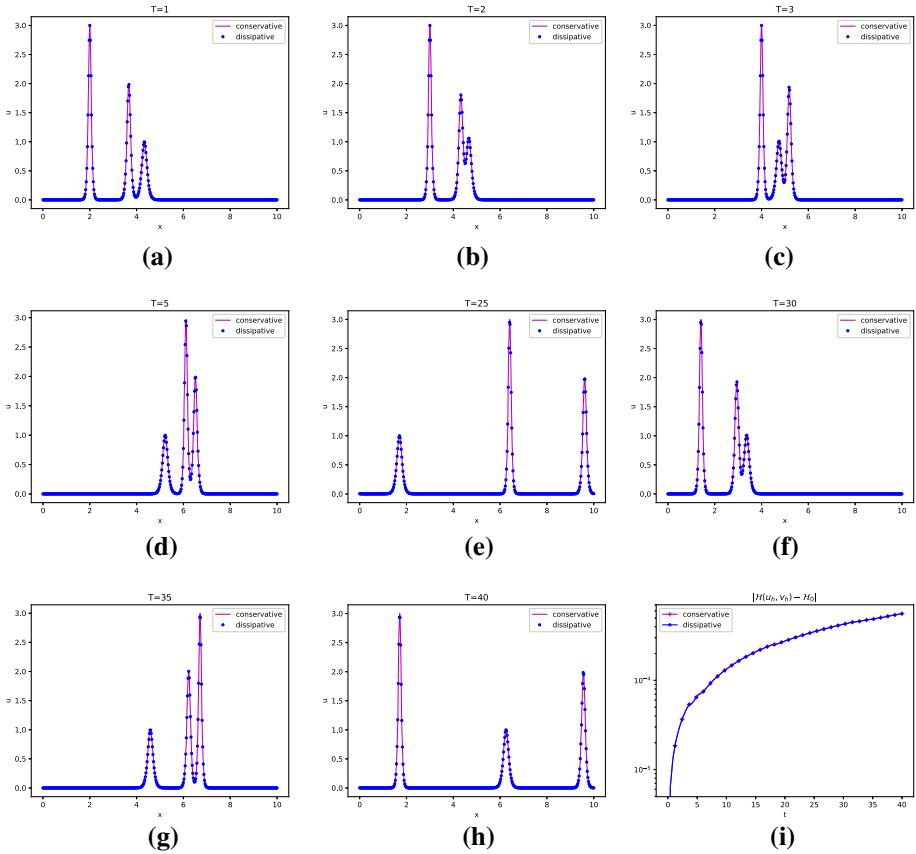


**Fig. 6** The interactions of three-solitary wave (6.5) with parameters (6.7),  $(x, t) \in [0, 10] \times [0, 40]$ .  $P^4$  elements and uniform mesh with  $N = 400$  cells. Fifth-order ARK method. **a–d** depict the first series of interactions; **e–h** depict interactions in a long time; **i** shows the  $\mathcal{H}$ -energy evolution in the semilog coordinate

this is an important property of interaction of multi-solitary waves which is consistent with the KdV equations. The information, such as amplitudes and shapes, about the separated solitons can be maintained well after each interaction in our methods, and this indicates the capability of schemes toward computing approximations of such solutions.

### 7 Conclusion

In this paper, we have developed several conservative and dissipative schemes for the KdV-type system (1.1). The stability analysis for the  $\mathcal{H}$ -conservative scheme and  $\mathcal{H}$ -stable schemes have been analyzed and the error estimates for two dissipative schemes with nonlinear terms taking different numerical fluxes are also given. Several numerical examples exhibiting various circumstances were shown to illustrate the accuracy and capability of these LDG schemes. Besides, these LDG schemes inherit the nice properties of DG methods on the flexibility for general geometry meshes, the  $hp$ -adaptivity and excellent parallel efficiency. Indeed, the the-

ory and supporting experiments presented herein strongly highlight the suitability of LDG techniques for approximating solutions of dispersive equations.

## Appendices

### A Proof of Lemma 4.4

**Proof** We separate the following proof into two parts according to the conservative and dissipative cases for  $\mathcal{I}$ .

- (The conservative case for  $\mathcal{I}_c$ )

$$\begin{aligned} \mathcal{I}_c(u_h, v_h) &= (2aA\mathcal{N}_c(u_h, u_h; u_h) + bD\mathcal{N}_c(u_h, u_h; u_h) + bC\mathcal{N}_c(v_h, v_h; v_h) + 2cF\mathcal{N}_c(v_h, v_h; v_h)) \\ &\quad + (bA\mathcal{N}_c(u_h, u_h; v_h) + 2cD\mathcal{N}_c(u_h, u_h; v_h) + 2aB\mathcal{N}_c(u_h, v_h; u_h) + bE\mathcal{N}_c(u_h, v_h; u_h)) \\ &\quad + (2aC\mathcal{N}_c(v_h, v_h; u_h) + bF\mathcal{N}_c(v_h, v_h; u_h) + bB\mathcal{N}_c(u_h, v_h; v_h) + 2cE\mathcal{N}_c(u_h, v_h; v_h)) \\ &:= (\mathcal{I}_{c,1}) + (\mathcal{I}_{c,2}) + (\mathcal{I}_{c,3}). \end{aligned} \tag{A.1}$$

With the conservative property  $\mathcal{N}_c(u, u; u) = 0$  given in (2.16), the first term  $(\mathcal{I}_{c,1}) = 0$ . By virtue of relations (2.14) and (2.15), and the conditions in (1.4), i.e.

$$\begin{aligned} 2Ba + (E - 2A)b - 4Dc &= 0, \\ 4Ca + (2F - B)b - 2Ec &= 0, \end{aligned}$$

the left two terms,  $(\mathcal{I}_{c,2})$  and  $(\mathcal{I}_{c,3})$ , satisfy

$$\begin{aligned} (\mathcal{I}_{c,2}) &= \frac{1}{2}(2ba + 4cD - 2aB - bE)\mathcal{N}_c(u_h, u_h; v_h) = 0, \\ (\mathcal{I}_{c,3}) &= \frac{1}{2}(4aC + 2bF - bB - 2cE)\mathcal{N}_c(v_h, v_h; u_h) = 0. \end{aligned}$$

- (The dissipative case for  $\mathcal{I}_d$ )

$$\begin{aligned} \mathcal{I}_d(u_h, v_h) &= (2aA\mathcal{N}_d(u_h, u_h; u_h) + bD\mathcal{N}_d(u_h, u_h; u_h) + bC\mathcal{N}_d(v_h, v_h; v_h) + 2cF\mathcal{N}_d(v_h, v_h; v_h)) \\ &\quad + (bA\mathcal{N}_d(u_h, u_h; v_h) + 2cD\mathcal{N}_d(u_h, u_h; v_h) + 2aB\mathcal{N}_d(u_h, v_h; u_h) + bE\mathcal{N}_d(u_h, v_h; u_h)) \\ &\quad + (2aC\mathcal{N}_d(v_h, v_h; u_h) + bF\mathcal{N}_d(v_h, v_h; u_h) + bB\mathcal{N}_d(u_h, v_h; v_h) + 2cE\mathcal{N}_d(u_h, v_h; v_h)) \\ &\quad + \frac{\varepsilon}{2} \sum_{j=1}^N (2a[u_h]^2 + 2b[u_h][v_h] + 2c[v_h]^2)_{j-\frac{1}{2}} \\ &:= (\mathcal{I}_{d,1}) + (\mathcal{I}_{d,2}) + (\mathcal{I}_{d,3}) + (\mathcal{I}_{d,4}). \end{aligned} \tag{A.2}$$

Applying the properties of  $\mathcal{N}_d$  in (2.25) and (2.26) and the conditions of  $a, b, c$  in (1.4),

$$\begin{aligned} 2Ba + (E - 2A)b - 4Dc &= 0, \\ 4Ca + (2F - B)b - 2Ec &= 0, \end{aligned}$$

hence  $(\mathcal{I}_{d1}), (\mathcal{I}_{d2})$  and  $(\mathcal{I}_{d3})$  become

$$(\mathcal{I}_{d,1}) = -\frac{1}{6}(2aA + bD) \sum_{j=1}^N ([u]^2[u])_{j-\frac{1}{2}} - \frac{1}{6}(bC + 2cF) \sum_{j=1}^N ([v]^2[v])_{j-\frac{1}{2}}$$

$$\geq -\frac{1}{3}(2aA + bD)\|u\|_\infty \sum_{j=1}^N ([u]^2)_{j-\frac{1}{2}} - \frac{1}{3}(bC + 2cF)\|v\|_\infty \sum_{j=1}^N ([v]^2)_{j-\frac{1}{2}}, \tag{A.3}$$

$$(\mathcal{I}_{d,2}) = -\frac{1}{2}(2cD + bA) \sum_{j=1}^N ([u]^2[v])_{j-\frac{1}{2}} \geq -(2cD + bA)\|v\|_\infty \sum_{j=1}^N ([u]^2)_{j-\frac{1}{2}}, \tag{A.4}$$

and

$$(\mathcal{I}_{d,3}) = -\frac{1}{2}(2aC + bF) \sum_{j=1}^N ([v]^2[u])_{j-\frac{1}{2}} \geq -(2aC + bF)\|u\|_\infty \sum_{j=1}^N ([v]^2)_{j-\frac{1}{2}}. \tag{A.5}$$

Combining the above three inequalities together, we have

$$\begin{aligned} & (\mathcal{I}_{d,1}) + (\mathcal{I}_{d,2}) + (\mathcal{I}_{d,3}) \\ & \geq -\left(\frac{1}{3}(2aA + bD)\|u\|_\infty + (2cD + bA)\|v\|_\infty\right) \sum_{j=1}^N ([u]^2)_{j-\frac{1}{2}} \\ & \quad - \left(\frac{1}{3}(bC + 2cF)\|v\|_\infty + (2aC + bF)\|u\|_\infty\right) \sum_{j=1}^N ([v]^2)_{j-\frac{1}{2}} \\ & = -\Lambda_1 \sum_{j=1}^N ([u]^2)_{j-\frac{1}{2}} - \Lambda_2 \sum_{j=1}^N ([v]^2)_{j-\frac{1}{2}}. \end{aligned} \tag{A.6}$$

Now we take into consideration of  $(\mathcal{I}_4)$  with the positive definite condition (1.5) which means there is a positive number  $\alpha$  such that  $\alpha(\xi^2 + \zeta^2) \leq a\xi^2 + b\xi\zeta + c\zeta^2$ , in detail

$$(\mathcal{I}_{d,4}) = \varepsilon \sum_{j=1}^N (a[u]^2 + b[u][v] + c[v]^2)_{j-\frac{1}{2}} \geq \varepsilon\alpha \sum_{j=1}^N ([u]^2 + [v]^2)_{j-\frac{1}{2}}. \tag{A.7}$$

Comparing (A.6) with (A.7), applying the additional conditions for the parameter  $\varepsilon$  that

$$\varepsilon \geq \frac{1}{\alpha} \max(|\Lambda_1|, |\Lambda_2|), \tag{A.8}$$

then we obtain the following inequality

$$\mathcal{I}_d(u_h, v_h) \geq -\Lambda_1 \sum_{j=1}^N ([u]^2)_{j-\frac{1}{2}} - \Lambda_2 \sum_{j=1}^N ([v]^2)_{j-\frac{1}{2}} + \varepsilon\alpha \sum_{j=1}^N ([u]^2 + [v]^2)_{j-\frac{1}{2}} \geq 0.$$

□

## B Proof of Lemma 4.5

**Proof** We separate the following proofs into two parts according to the conservative and dissipative cases for  $\mathcal{J}$ .

- (The conservative case for  $\mathcal{J}_C$ ). Take account of the Eqs. (3.4), (3.5) by choosing the test functions as follows

$$\xi_1 = q_h^{(u)}, \quad \zeta_1 = -p_h^{(u)}. \tag{B.1}$$

Combine (3.4) and (3.5) together, sum up over  $j$  and take into consideration of the periodic condition, then we have

$$\begin{aligned} & \sum_{j=1}^N (p_h^{(u)}, q_h^{(u)})_{I_j} + \sum_{j=1}^N (q_h^{(u)}, (q_h^{(u)})_x)_{I_j} + \sum_{j=1}^N (\widehat{q}_h^{(u)} [q_h^{(u)}])_{j-\frac{1}{2}} \\ & + \sum_{j=1}^N (q_h^{(u)}, -p_h^{(u)})_{I_j} + \sum_{j=1}^N (u_h, (-p_h^{(u)})_x)_{I_j} + \sum_{j=1}^N (\widehat{u}_h [-p_h^{(u)}])_{j-\frac{1}{2}} = 0. \end{aligned} \tag{B.2}$$

Noticing that the first term can eliminate the forth term, and recalling the choice of the numerical flux  $\widehat{q}_h^{(u)} = \{q_h^{(u)}\}$  with the property  $\mathcal{D}^*(q_h^{(u)}, q_h^{(u)}) = 0$  in (2.34), namely

$$\sum_{j=1}^N \left( (q_h^{(u)}, (q_h^{(u)})_x)_{I_j} + (\{q_h^{(u)}\} [q_h^{(u)}])_{j-\frac{1}{2}} \right) = 0, \tag{B.3}$$

then we can simplify the Eq. (B.2) into

$$\mathcal{D}^*(u_h, p_h^{(u)}) = - \sum_{j=1}^N (u_h, (p_h^{(u)})_x)_{I_j} - \sum_{j=1}^N (\{u_h\} [p_h^{(u)}])_{j-\frac{1}{2}} = 0. \tag{B.4}$$

Herein we use the form  $\mathcal{D}^*$  defined in (2.29) introduced for the reason of concision. The same procedure can also be applied in (3.7) and (3.8) with taking test functions as

$$\xi_2 = q_h^{(v)}, \quad \zeta_2 = -p_h^{(v)}, \tag{B.5}$$

then we get

$$\mathcal{D}^*(v_h, p_h^{(v)}) = - \sum_{j=1}^N (v_h, (p_h^{(v)})_x)_{I_j} - \sum_{j=1}^N (\{v_h\} [p_h^{(v)}])_{j-\frac{1}{2}} = 0. \tag{B.6}$$

Next we retake the test functions in (3.4), (3.5), (3.7) and (3.8) as

$$\xi_1 = q_h^{(v)}, \quad \zeta_1 = -p_h^{(v)}, \quad \xi_2 = q_h^{(u)}, \quad \zeta_2 = -p_h^{(u)}, \tag{B.7}$$

then combine four equations together

$$\begin{aligned} & \sum_{j=1}^N (p_h^{(u)}, q_h^{(v)})_{I_j} + \sum_{j=1}^N (q_h^{(u)}, -p_h^{(v)})_{I_j} + \sum_{j=1}^N (p_h^{(v)}, q_h^{(u)})_{I_j} + \sum_{j=1}^N (q_h^{(v)}, -p_h^{(u)})_{I_j} \\ & + \sum_{j=1}^N (q_h^{(u)}, (q_h^{(v)})_x)_{I_j} + \sum_{j=1}^N (q_h^{(v)}, (q_h^{(u)})_x)_{I_j} \\ & + \sum_{j=1}^N (\widehat{q}_h^{(u)} [q_h^{(v)}])_{j-\frac{1}{2}} + \sum_{j=1}^N (\widehat{q}_h^{(v)} [q_h^{(u)}])_{j-\frac{1}{2}} \end{aligned}$$

$$\begin{aligned}
 & - \sum_{j=1}^N \left( u_h, (p_h^{(v)})_x \right)_{I_j} - \sum_{j=1}^N \left( \widehat{u}_h [p_h^{(v)}] \right)_{j-\frac{1}{2}} - \sum_{j=1}^N \left( v_h, (p_h^{(u)})_x \right)_{I_j} \\
 & - \sum_{j=1}^N \left( \widehat{v}_h [p_h^{(u)}] \right)_{j-\frac{1}{2}} = 0.
 \end{aligned} \tag{B.8}$$

Obviously, the first four terms cancel out immediately. With definitions of  $\widehat{q}_h^{(u)}$  and  $\widehat{q}_h^{(v)}$  and the equality  $\mathcal{D}^*(q_h^{(u)}, q_h^{(v)}) + \mathcal{D}^*(q_h^{(v)}, q_h^{(u)}) = 0$ , the second four terms also vanish, i.e.

$$\begin{aligned}
 & \sum_{j=1}^N \left( q_h^{(u)}, (q_h^{(v)})_x \right)_{I_j} + \sum_{j=1}^N \left( \widehat{q}_h^{(u)} [q_h^{(v)}] \right)_{j-\frac{1}{2}} \\
 & + \sum_{j=1}^N \left( q_h^{(v)}, (q_h^{(u)})_x \right)_{I_j} + \sum_{j=1}^N \left( \widehat{q}_h^{(v)} [q_h^{(u)}] \right)_{j-\frac{1}{2}} = 0.
 \end{aligned} \tag{B.9}$$

Thus it leads to another identity

$$\begin{aligned}
 & \mathcal{D}^*(u_h, p_h^{(v)}) + \mathcal{D}^*(v_h, p_h^{(u)}) \\
 & = - \sum_{j=1}^N \left( u_h, (p_h^{(v)})_x \right)_{I_j} - \sum_{j=1}^N \left( v_h, (p_h^{(u)})_x \right)_{I_j} \\
 & \quad - \sum_{j=1}^N \left( \{u_h\} [p_h^{(v)}] \right)_{j-\frac{1}{2}} - \sum_{j=1}^N \left( \{v_h\} [p_h^{(u)}] \right)_{j-\frac{1}{2}} \\
 & = 0.
 \end{aligned} \tag{B.10}$$

In summary, by virtue of the definition of  $\mathcal{D}^*$ , equalities in (B.4), (B.6) and (B.10) can be rewritten into the following concise forms

$$\begin{aligned}
 & \mathcal{D}^*(u_h, p_h^{(u)}) = 0, \\
 & \mathcal{D}^*(v_h, p_h^{(v)}) = 0, \\
 & \mathcal{D}^*(u_h, p_h^{(v)}) + \mathcal{D}^*(v_h, p_h^{(u)}) = 0,
 \end{aligned} \tag{B.11}$$

Now, on account of the property of  $\mathcal{D}^*(\xi, \zeta)$ , namely

$$\mathcal{D}^*(\xi, \zeta) + \mathcal{D}^*(\zeta, \xi) = 0,$$

and adding  $2a\mathcal{D}^*(u_h, p_h^{(u)}) + b(\mathcal{D}^*(u_h, p_h^{(v)}) + \mathcal{D}^*(v_h, p_h^{(u)})) + 2c\mathcal{D}^*(v_h, p_h^{(v)}) = 0$  to  $\mathcal{J}_c$ , then we have

$$\mathcal{J}_c(u_h, v_h; p_h^{(u)}, p_h^{(v)}) = 0.$$

- (The dissipative case for  $\mathcal{J}_d$ ) Using the similar strategies as in the last conservative case, the different choices of numerical fluxes

$$\widehat{p}_h^{(\chi)} = (p_h^{(\chi)})^+, \quad \widehat{q}_h^{(\chi)} = (q_h^{(\chi)})^+, \quad \widehat{\chi}_h = \chi_h^-,$$

directly result in some inequalities comparing to the equalities in (B.11)

$$\mathcal{D}^-(u_h, p_h^{(u)}) \leq 0,$$

$$\begin{aligned} \mathcal{D}^-(v_h, p_h^{(v)}) &\leq 0, \\ \mathcal{D}^-(u_h, p_h^{(v)}) + \mathcal{D}^-(v_h, p_h^{(u)}) &\leq 0. \end{aligned} \quad (\text{B.12})$$

On account of the property,  $\mathcal{D}^-(\xi, \zeta) + \mathcal{D}^+(\zeta, \xi) = 0$ , and the conditions  $a, c > 0$  together with the extra assumption  $b \geq 0$ , then we have

$$\begin{aligned} \mathcal{J}_d(u_h, v_h; p_h^{(u)}, p_h^{(v)}) &= 2a\mathcal{D}^+(p_h^{(u)}, u_h) + b(\mathcal{D}^+(p_h^{(u)}, v_h) + \mathcal{D}^+(p_h^{(v)}, u_h)) + 2c\mathcal{D}^+(p_h^{(v)}, v_h) \\ &= -(2a\mathcal{D}^-(u_h, p_h^{(u)}) + b(\mathcal{D}^-(u_h, p_h^{(v)}) + \mathcal{D}^-(v_h, p_h^{(u)})) + 2c\mathcal{D}^-(v_h, p_h^{(v)})) \geq 0. \end{aligned}$$

□

## References

- Ash, J.M., Cohen, J., Wang, G.: On strongly interacting internal solitary waves. *J. Fourier Anal. Appl.* **2**(5), 507–517 (1995)
- Bassi, F., Rebay, S.: A high-order accurate discontinuous finite element method for the numerical solution of the compressible Navier–Stokes equations. *J. Comput. Phys.* **131**(2), 267–279 (1997)
- Bona, J., Chen, H., Karakashian, O., Xing, Y.: Conservative, discontinuous Galerkin-methods for the generalized Korteweg–de Vries equation. *Math. Comput.* **82**(283), 1401–1432 (2013)
- Bona, J.L., Chen, H., Karakashian, O.: Stability of solitary-wave solutions of systems of dispersive equations. *Appl. Math. Optim.* **75**(1), 27–53 (2017)
- Bona, J.L., Chen, H., Karakashian, O., Wise, M.M.: Finite element methods for a system of dispersive equations. *J. Sci. Comput.* **77**(3), 1371–1401 (2018)
- Bona, J.L., Smith, R.: The initial-value problem for the Korteweg–de Vries equation. *Phil. Trans. R. Soc. Lond. A* **278**(1287), 555–601 (1975)
- Cheng, Y., Shu, C.-W.: A discontinuous Galerkin finite element method for time dependent partial differential equations with higher order derivatives. *Math. Comput.* **77**(262), 699–730 (2008)
- Christopher, K.A., Mark, C.H.: Additive Runge–Kutta schemes for convection–diffusion–reaction equation. *Appl. Numer. Math.* **44**(1–2), 139–181 (2003)
- Ciarlet, P.G.: *The Finite Element Method for Elliptic Problems*. SIAM, New York (2002)
- Cockburn, B., Shu, C.-W.: The local discontinuous Galerkin method for time-dependent convection–diffusion systems. *SIAM J. Numer. Anal.* **35**(6), 2440–2463 (1998)
- Cohen, J., Wang, G., et al.: Global well-posedness for a system of KdV-type equations with coupled quadratic nonlinearities. *Nagoya Math. J.* **215**, 67–149 (2014)
- Colliander, J., Keel, M., Staffilani, G., Takaoka, H., Tao, T.: Sharp global well-posedness for KdV and modified KdV on  $\mathbb{R}$  and  $\mathbb{T}$ . *J. Am. Math. Soc.* **16**(3), 705–749 (2003)
- Harten, A.: High resolution schemes for hyperbolic conservation laws. *J. Comput. Phys.* **49**(3), 357–393 (1983)
- Hou, S., Liu, X.-D.: Solutions of multi-dimensional hyperbolic systems of conservation laws by square entropy condition satisfying discontinuous Galerkin method. *J. Sci. Comput.* **31**(1–2), 127–151 (2007)
- Karakashian, O., Makridakis, C.: A posteriori error estimates for discontinuous Galerkin methods for the generalized Korteweg–de Vries equation. *Math. Comput.* **84**(293), 1145–1167 (2015)
- Karakashian, O., Xing, Y.: A posteriori error estimates for conservative local discontinuous Galerkin methods for the generalized Korteweg–de Vries equation. *Commun. Comput. Phys.* **20**(1), 250–278 (2016)
- Li, X., Xing, Y., Chou, C.: Optimal energy conserving and energy dissipative local discontinuous Galerkin methods for the Benjamin–Bona–Mahony equation. *J. Sci. Comput.* **83**(1), 17 (2020)
- Luo, J., Shu, C.-W., Zhang, Q.: A priori error estimates to smooth solutions of the third order Runge–Kutta discontinuous Galerkin method for symmetrizable systems of conservation laws. *ESAIM Math. Model. Numer. Anal.* **49**(4), 991–1018 (2015)
- Roe, P.L.: Approximate Riemann solvers, parameter vectors, and difference schemes. *J. Comput. Phys.* **43**(2), 357–372 (1981)
- Xia, Y., Xu, Y., Shu, C.-W.: Efficient time discretization for local discontinuous Galerkin methods. *Discrete Continuous Dyn. Syst. Ser. B* **8**(3), 677 (2007)

21. Xu, Y., Shu, C.-W.: Local discontinuous Galerkin methods for two classes of two-dimensional nonlinear wave equations. *Physica D* **208**(1–2), 21–58 (2005)
22. Xu, Y., Shu, C.-W.: Error estimates of the semi-discrete local discontinuous Galerkin method for nonlinear convection–diffusion and KdV equations. *Comput. Methods Appl. Mech. Eng.* **196**(37), 3805–3822 (2007)
23. Xu, Y., Shu, C.-W.: A local discontinuous Galerkin method for the Camassa–Holm equation. *SIAM J. Numer. Anal.* **46**(4), 1998–2021 (2008)
24. Xu, Y., Shu, C.-W.: Local discontinuous Galerkin method for the Hunter–Saxton equation and its zero-viscosity and zero-dispersion limits. *SIAM J. Sci. Comput.* **31**(2), 1249–1268 (2008)
25. Xu, Y., Shu, C.-W.: Dissipative numerical methods for the Hunter–Saxton equation. *J. Comput. Math.* **28**, 606–620 (2010)
26. Xu, Y., Shu, C.-W.: Local discontinuous Galerkin methods for high-order time-dependent partial differential equations. *Commun. Comput. Phys.* **7**(1), 1 (2010)
27. Yan, J., Shu, C.-W.: A local discontinuous Galerkin method for KdV type equations. *SIAM J. Numer. Anal.* **40**(2), 769–791 (2002)
28. Zhang, C., Xu, Y., Xia, Y.: Local discontinuous Galerkin methods for the  $\mu$ -Camassa–Holm and  $\mu$ -Degasperis–Procesi equations. *J. Sci. Comput.* **376**, 112857 (2005)
29. Zhang, Q., Shu, C.-W.: Error estimates to smooth solutions of Runge–Kutta discontinuous Galerkin methods for scalar conservation laws. *SIAM J. Numer. Anal.* **42**(2), 641–666 (2004)
30. Zhang, Q., Shu, C.-W.: Error estimates to smooth solutions of Runge–Kutta discontinuous Galerkin method for symmetrizable systems of conservation laws. *SIAM J. Numer. Anal.* **44**(4), 1703–1720 (2006)
31. Zhang, Q., Xia, Y.: Conservative and dissipative local discontinuous Galerkin methods for Korteweg–de Vries type equations. *Commun. Comput. Phys.* **25**(2), 532–563 (2019)

**Publisher's Note** Springer Nature remains neutral with regard to jurisdictional claims in published maps and institutional affiliations.